species raises the possibility of the occurrence of either sequential or simultaneous loss of two solvent molecules from $[M(solvent)_6]^{2+}$, both of which provide D pathways for solvent exchange on $[M(solvent)_6]^{2+}$. Evidence for the sequential loss of two solvent molecules from $[NiL(solvent)_2]^{2+}$ (where L is a tetradentate ligand) has been presented,[29,30] and while no direct evidence is available for such a process occurring on $[M(solvent)_6]^{2+}$, it presents no conceptual difficulties. The simultaneous loss of two solvent molecules from $[M(solvent)_6]^{2+}$ to produce tetrahedral $[M(solvent)_4]^{2+}$ could be envisaged to involve the simultaneous departure of two trans solvent molecules along the C_4 axis of $[M(solvent)_6]^{2+}$ while the two remaining pairs of cis solvent molecules contrarotate about a common C_2 axis as their bond angles increase from 90 to 109.5°. (A square-planar product is more simply obtained by omission of the contrarotation of the cis pairs.) The reverse process requires a reactive three-body collision. Unless there is a highly concerted involvement of solvent both in and outside the first coordination spheres (as a recently published computer modeling of solvent exchange suggests is the case for exchange of a single solvent molecule[31]), the simultaneous process would seem to be less favored than the sequential process, but the available data provide no basis for a definitive choice between the two processes. Nevertheless, this study clearly demonstrates that an increase in crowding at the metal center in $[M(solvent)_6]^{2+}$ not only labilizes the solvent for a d-activated mechanism when M = Ni or Co but also in the case of the latter metal causes the mechanism to change from I_d to D when the solvent is changed from dmf[5] to dma or def.

It is appropriate to compare the findings of this study with those from other studies in which the nature of the solvent was varied. Dma exchange on $[Sc(dma)_6]^{3+}$ in acetonitrile diluent is characterized by first- and second-order exchange processes, respectively, assigned to D and A mechanisms, whereas the exchange of dmf and def on scandium(III) is found to be too fast for determination by NMR methods.[10] This increased lability is thought to be a consequence of either the less sterically crowding dmf and def facilitating very rapid solvent exchange on $[Sc(solvent)_6]^{3+}$ through an A mechanism or the formation of very labile $[Sc(solvent)_7]^{3+}$. Evidence for the labilization of $[M(solvent)_n]^{3+}$ with an increase in n may be adduced from the observation that $k(298.2\ K) = 3.1 \times 10^7\ s^{-1}$ for $[Tm(dmf)_8]^{3+}$[32] whereas for $[Tm(tmu)_6]^{3+}$[33] $k(298.2\ K) = 145\ s^{-1}$ where tmu = 1,1,3,3-tetramethylurea (D_N = 29.6), both of which undergo exchange through a D mechanism. However, a change in coordination number may also result in a change in mechanism, as exemplified by $[UO_2(OP(NMe_2)_3)_4]^{2+}$, for which the predominant solvent-exchange process occurs through an A mechanism, and $[UO_2(OP(OMe)_3)_5]^{2+}$, for which a D mechanism operates.[3,4]

Acknowledgment. We thank the Australian Research Grants Scheme for partially supporting this research.

Registry No. def, 617-84-5; dma, 127-19-5; $[Co(def)_6]^{2+}$, 100485-68-5; $[Ni(def)_6]^{2+}$, 45318-23-8; $[Co(dma)_6]^{2+}$, 38213-56-8; $[Ni(dma)_6]^{2+}$, 48077-69-6.

(29) Coates, J. H.; Hadl, D. A.; Lincoln, S. F.; Dodgen, H. W.; Hunt, J. P. *Inorg. Chem.* **1981**, *20*, 707–711.
(30) Sachinidis, J.; Grant, M. W. *J. Chem. Soc., Chem. Commun.* **1978**, 157–158.
(31) Connick, R. E.; Alder, B. J. *J. Phys. Chem.* **1983**, *87*, 2764–2771.
(32) Pisaniello, D. L.; Helm, L.; Meier, P.; Merbach, A. E. *J. Am. Chem. Soc.* **1983**, *105*, 4528–4536.
(33) Lincoln, S. F.; White, A., unpublished data.

Contribution from the Department of Chemistry, The University of North Carolina, Chapel Hill, North Carolina 27514

Mechanism of Reduction of Bound Nitrite to Ammonia

W. Rorer Murphy, Jr., Kenneth Takeuchi, Mark H. Barley, and Thomas J. Meyer*

Received October 9, 1985

Electrochemical experiments on the oxidation of $[(tpy)(bpy)M(NH_3)]^{2+}$ (M = Ru, Os; tpy = 2,2′,2″-terpyridine; bpy = 2,2′-bipyridine) and reduction of $[(tpy)(bpy)M(NO_2)]^{+}$ have given insight into the mechanistic details of how bound nitrite is converted into ammonia. A critical feature is acid–base interconversion to the nitrosyl form, $[(tpy)(bpy)M(NO)]^{3+}$, which undergoes a series of stepwise, one-electron reductions. Direct experimental evidence has been obtained for a series of intermediates that can be formulated as $[(tpy)(bpy)M^{IV}(NH)]^{2+}$, $[(tpy)(bpy)M^{V}(N)]^{2+}$ or $[(tpy)(bpy)M^{II}(NH_2O)]^{2+}$, $[(tpy)(bpy)M^{II}(NHO)]^{2+}$, and $[(tpy)(bpy)M^{II}(NO\cdot)]^{2+}$.

In the overall reduction of nitrate to ammonia in green plants[1–4] an important step is the six-electron reduction of nitrite to ammonia. The reduction is catalyzed by the enzyme nitrite reductase, which is a complex protein consisting of an iron–sulfur unit and an iron–isobacteriochlorin group or siroheme. In the enzyme it appears that the iron–sulfur unit accepts electrons from reduced ferredoxin and subsequently transfers them to the siroheme site,[1] which is also the binding site for the nitrite ion. Two remarkable features of the enzymatic reduction are that it is facile even though six-electron in nature and that no evidence has been obtained for intermediate stages in the reduction.

Results have been reported on attempts to model the active site of nitrite reductase via synthetically accessible isobacteriochlorins.[5–7] In addition, certain features of the reactivity of the enzyme have been observed in simple metal complexes, most notably by Armor and co-workers, who found that $[(NH_3)_5Ru(NO)]^{3+}$ is reduced quantitatively[8] to $[(NH_3)_6Ru]^{2+}$ by Cr(II) and that $[(NH_3)_6Ru]^{2+}$ is oxidized in 30% yield to $[(NH_3)_5Ru(NO)]^{3+}$ by O_2 in basic solution.[9] More recently, Bottomley and Mukaida have shown that $[(py)_4Ru(NO)Cl]^{2+}$ (py = pyridine) undergoes two reversible one-electron reductions, followed by an irreversible four-electron reduction to give $[(py)_4Ru(NH_3)Cl]^{+}$.[10] It has also been reported[11] that $[(tpy)(bpy)Ru(NH_3)]^{2+}$ (tpy = 2,2′,2″-terpyridine; bpy = 2,2′-bipyridine) is rapidly and quantitatively oxidized to give $[(tpy)(bpy)Ru(NO)]^{3+}$, which is in

(1) Losada, M. *J. Mol. Catal.* **1975/76**, *1*, 245.
(2) Losada, M. *J. Electroanal. Chem. Interfacial Electrochem.* **1979**, *104*, 205.
(3) Candan, P.; Manzano, C.; Losada, M. *Nature (London)* **1976**, *262*, 715.
(4) Murphy, M. J.; Siegel, L. M.; Tove, S. R.; Kamin, H. *Proc. Natl. Acad. Sci. U.S.A.* **1974**, *71*, 612.
(5) Chang, C. K.; Hanson, L. K.; Richards, P. F.; Yound, R.; Fajer, J. *Proc. Natl. Acad. Sci. U.S.A.* **1981**, *78*, 2652.
(6) Stolzenberg, A. M.; Strauss, S. H.; Holm, R. H. *J. Am. Chem. Soc.* **1981**, *103*, 4763.
(7) Barkigia, K. M.; Fajer, J.; Spaulding, L. D.; Williams, G. J. B. *J. Am. Chem. Soc.* **1981**, *103*, 176.
(8) (a) Armor, J. N.; Hoffman, M. Z. *Inorg. Chem.* **1975**, *14*, 444. (b) Armor, J. N. *Inorg. Chem.* **1973**, *12*, 1959. (c) Armor, J. N.; Frank, S., private communication.
(9) Pell, S. D.; Armor, J. N. *J. Am. Chem. Soc.* **1975**, *97*, 5012.
(10) Bottomley, F.; Mukaida, M. *J. Chem. Soc., Dalton Trans.* **1982**, 1933.
(11) (a) Thompson, M. S.; Meyer, T. J. *J. Am. Chem. Soc.* **1981**, *103*, 5577. (b) Thompson, M. S. Ph.D. Dissertation, The University of North Carolina, 1981.

0020-1669/86/1325-1041$01.50/0

acid–base equilibrium with the corresponding nitro complex.[12]

We report here in greater detail on our initial observation[13] that the nitrosyl group when bound in polypyridyl complexes of Ru or Os can undergo a chemically reversible reduction to coordinated ammonia. From our work and the earlier work mentioned above, it is possible to develop a detailed mechanism for the interconversion of nitrite and ammonia. This mechanism may also have relevance both for the enzymatic system and for the net electrochemical reduction of nitrite to NH_3 based on the water-soluble, tetrasulfonated Fe(III) complex of tetraphenylporphine.[13]

Experimental Section

Locally deionized water was used. Acetonitrile was purchased from Burdick and Jackson (UV grade) and stored over 4-Å molecular sieves (Davison), which were activated by washing with water to remove particulate matter and dried for 24 h at 350 °C in a muffle furnace.

The supporting electrolytes for electrochemistry in acetonitrile were either tetrabutylammonium hexafluorophosphate (TBAH) or tetraethylammonium perchlorate (TEAP) in 0.1 M concentrations. TBAH was prepared by dissolving tetrabutylammonium bromide (Fisher Scientific) in hot water, adding 1.2 equiv of 70% HPF_6 (Alfa Chemicals), heating at reflux for 20 min, to remove HBr, and cooling. The resulting precipitate was collected by filtration, recrystallized at least three times from ethanol (acidified with HPF_6), and dried in a vacuum oven at 100 °C for 8 h. TEAP, $[NEt_4]ClO_4$, was prepared in a similar fashion from tetraethylammonium bromide (Fisher Scientific) and 70% $HClO_4$ (Mallinckrodt) with use of water as both the preparation and crystallization solvent.

The supporting electrolytes for electrochemistry in aqueous solution consisted of sulfuric acid in appropriate concentrations (for pH values below 2) or conjugate acid–base pairs as buffers (0.05 M). The buffered solutions were 0.1 M in Na_2SO_4 in order to suppress specific ion effects. The buffers were made from potassium acid phthalate (KHP), KH_2PO_4, Na_3PO_4, H_3PO_4, H_2SO_4, and NaOH. The phosphate salts and NaOH were purchased from Fisher Scientific. The pH's of the solutions were measured by using a Radiometer PHM62 meter equipped with separate glass and calomel electrodes. All other reagents were used as received.

Preparations. $[(tpy)(bpy)Ru(NO_2)](BF_4)$ was prepared by a modification of a previously published procedure.[14] $[(tpy)(bpy)RuCl]Cl$[14] (1.20 g) was dissolved in 200 mL of 1:4 ethanol/water. $NaNO_2$ (1.4 g) was added and the solution heated at reflux for 3.5 h. The solution was cooled, and $NaBF_4$ (8.4 g) was added. The solution was concentrated on a rotary evaporator until small red crystals formed in the solution. The solution was refrigerated for 3.5 h and filtered to isolate the red crystals. The crystals were washed with ice-cold water and dried in a vacuum desiccator. The yield was 88%. Anal. Calcd for $[(tpy)(bpy)Ru(NO_2)](BF_4)\cdot H_2O$: C, 48.82; H, 3.19; N, 13.19. Found: C, 48.07; H, 3.12; N, 13.26.

$[(tpy)(bpy)Ru(NO)](BF_4)_3$. $[(tpy)(bpy)Ru(NO_2)](BF_4)\cdot H_2O$ (ca. 0.1 g) was suspended in ca. 20 mL of stirring methanol with glass beads added to the solution. HBF_4 (40%) was added dropwise until the suspended particles turned from red to yellow. The suspension was stirred for 20 min or until all of the red particles turned yellow. The yellow precipitate was collected by filtration and washed with methanol. The yellow powder was dissolved in a minimum amount of acetonitrile, and the solution was filtered and added dropwise to stirring diethyl ether. The precipitate was collected by filtration and dried in a vacuum desiccator. Anal. Calcd for $[(tpy)(bpy)Ru(NO)](BF_4)_3\cdot H_2O$: C, 37.58; H, 2.65; N, 10.52. Found: C, 36.82; H, 2.68; N, 10.23.

$[(tpy)(bpy)Ru(NH_3)]^{2+}$ was synthesized in situ by reducing $[(tpy)(bpy)Ru(NO)]^{3+}$ in 0.1 M H_2SO_4 or pH 3.7 media (0.05 M KHP and 0.1 M Na_2SO_4) with a Hg-pool electrode. The product was identified by comparison of the characteristic redox potential and visible absorption maximum (λ_{max}) with values obtained for an authentic sample.[11b]

$[(tpy)(bpy)Os(NH_3)](PF_6)_2$. $[(tpy)(bpy)Os(NO)](PF_6)_3$[15] (~75 mg) was dissolved in 20 mL of water. To this solution was added 150 mg of zinc powder followed by 5 drops of concentrated HCl every 5 min for 25 min with vigorous stirring. After this addition the solution was stirred for a further 5 min before filtering. To the filtrate was added 2 mL of saturated aqueous NH_4PF_6, and the precipitated product was collected; yield 60 mg. Anal. Calcd for $[(tpy)(bpy)Os(NH_3)](PF_6)_2$: C, 33.78; H, 2.54; N, 9.61. Found: C, 33.86; H, 2.50; N, 9.48.

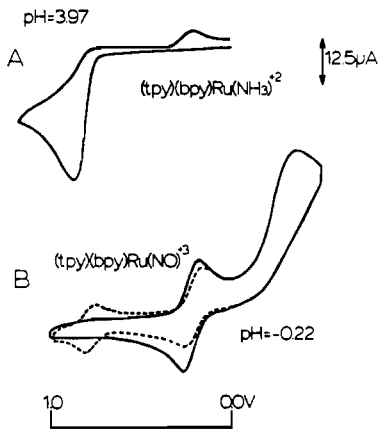

Figure 1. Cyclic voltammograms of (A) $[(tpy)(bpy)Ru(NH_3)]^{2+}$ in pH 3.97 media (0.1 M Na_2SO_4, 0.1 M KHP, and a small amount of NaOH) at a carbon-paste electrode and (B) $[(tpy)(bpy)Ru(NO)]^{3+}$ in 1 M H_2SO_4 at a glassy-carbon electrode. The solid line is the first scan, starting at 0.00 V and sweeping positively, then negatively, and back to 0.00 V. The dashed line is the continuation of the positive sweep. The scan rate is 100 mV/s.

$[(bpy)_2Ru(NO)Cl](PF_6)_2$,[12b] $[(bpy)_2Ru(NO_2)(NO)](PF_6)_2$,[12b] $[(bpy)_2Ru(NO)(py)](PF_6)_3$,[12b] $[(tpy)(bpy)Os(NO_2)](PF_6)$,[15] and $[(tpy)(bpy)Os(NO)](PF_6)_3$[15] were synthesized by using previously reported procedures.

Ultraviolet–visible measurements were made on a Varian Model 634 spectrometer. A Princeton Applied Research (PAR) Model 173 potentiostat/galvanostat with a PAR Model 179 digital coulometer was used for cyclic voltammetry and coulometry experiments. The triangle waveforms were generated with a PAR Model 175 universal programmer. Differential pulse voltammograms were measured with a PAR Model 174A polarographic analyzer. The current–time or current–potential curves were recorded on a Hewlett-Packard Model 7015B X-Y recorder with the input filters engaged to reject 60-Hz noise. At scan rates greater than 200 mV/s, a Textronix Model 564B storage oscilloscope was used to record the current–potential curves.

A saturated sodium chloride calomel electrode (SSCE, +0.234 V vs. NHE)[16] and a platinum auxiliary electrode were used in all electrochemical measurements. Disk electrodes of platinum (Englehardt Industries) and glassy carbon (VT-10, Atomergic Chemetals) of local design[17] and construction were used for cyclic and differential pulse voltammetry in acetonitrile and water, respectively. The electrodes were cleaned before each measurement by polishing at high speed with 1-μm alumina slurried with water and 1-μm diamond paste slurried with diamond paste extender or an 8-in. Microcloth pad mounted on an 8-in. polisher. All polishing supplies and equipment were purchased from Buehler, Ltd. The polishing media were removed from the electrodes by sonicating them in deionized water with a Branson Model B22-4 ultrasonic cleaner.

Carbon-paste electrodes were constructed in the following manner. Acheson grade 38 graphite (Fisher Scientific) was mixed with IR grade Nujol (Aldrich Chemical Co.) in a ratio of 15 g of graphite to 9 mL of Nujol.[18a] A glass tube (ca. 4 mm inner diameter) was pressed into the paste and the paste firmly packed with a glass rod until ca. 3 cm of paste was in the tube. A copper wire that had been cleaned with nitric acid was pressed into the back of the paste plug to make electrical contact. The surface of the electrode was smoothed flat with a piece of weighing paper, the electrode placed in the aqueous electrolyte solution without anolyte, and the potential cycled between the solvent limits until a smooth background was observed.

Platinum-gauze electrodes of high surface area were used as the working electrodes for bulk electrolyses in acetonitrile. A mercury-pool electrode was used as the working electrode for aqueous reductions and a reticulated vitreous carbon electrode (ERG Industries) for aqueous

(12) (a) Meyer, T. J.; Godwin, J. B.; Winterton, N. *J. Chem. Soc. D* **1970**, 872. (b) Godwin, J. B.; Meyer, T. J. *Inorg. Chem.* **1971**, *10*, 2150.
(13) (a) Murphy, W. R., Jr.; Takeuchi, K. J.; Meyer, T. J. *J. Am. Chem. Soc.* **1982**, *104*, 5817. (b) Barley, M. H.; Takeuchi, K. J.; Murphy, W. R., Jr.; Meyer, T. J. *J. Chem. Soc., Chem. Commun.* **1985**, 507.
(14) Sullivan, B. P.; Calvert, J. M.; Meyer, T. J. *Inorg. Chem.* **1980**, *19*, 1404.
(15) Pipes, D. W.; Meyer, T. J. *Inorg. Chem.* **1984**, *23*, 2466.
(16) Bard, A. J.; Faulkner, L. R. "Electrochemical Methods"; Wiley: New York, 1980; end pages.
(17) Martin, G. W. Ph.D. Dissertatiion, The University of North Carolina, 1978.
(18) (a) Adams, R. N. "Electrochemistry at Solid Electrodes"; Marcel Dekker: New York, 1969; pp 280–283. (b) *Ibid.*, pp 141–143. (c) Sawyer, D. T.; Roberts, J. L., Jr. "Experimental Electrochemistry for Chemists"; Wiley: New York, 1974; p 90.

Table I. Reduction Potentials at Room Temperature in Acetonitrile and Water vs. the Saturated Calomel Electrode

couple	$E_{1/2}$, V	
	H_2O	CH_3CN
$[(tpy)(bpy)Os(NO_3)]^{2+/+}$		0.60[a]
$[(tpy)(bpy)Ru(NO_3)]^{2+/+}$		0.96[b]
$[(tpy)(bpy)Os(NO_2)]^{2+/+}$	0.60	0.71
$[(tpy)(bpy)Ru(NO_2)]^{2+/+}$	0.93	1.05 (E_p^a)
$[(tpy)(bpy)Os(NH_3)]^{3+/2+}$	0.41[c]	0.69
$[(tpy)(bpy)Ru(NH_3)]^{3+/2+}$	0.78[d]	1.04[e]
$[(tpy)(bpy)Ru(NCCH_3)]^{3+/2+}$		1.26[b]
$[(tpy)(bpy)Ru(NO)]^{3+/2+}$ (A)[f]	0.23	0.45
E_p^c(B)[f]	−0.36[g]	−0.25
$[(tpy)(bpy)Os(NO)]^{3+/2+}$ (A)	−0.20	−0.02
E_p^c(B)	−0.51[h]	−0.24

[a] Taken from ref 15. [b] Calvert, J. M. unpublished observation. [c] The wave is reversible only below pH 6. [d] The wave is reversible only below pH 2. [e] Taken from ref 14. [f] Note the labeling scheme in Figure 5. [g] Potential at peak current for the second reduction wave at pH 4.68 in Figure 5. [h] Potential at peak current for the second reduction wave at pH 9.15 in Figure 9.

oxidations. The cells used in this work are described in ref 19.

Results

Interconversion of Coordinated Nitrite (Nitrosyl) and Ammonia: Net Reactions. The voltammograms in Figure 1 illustrate the facile interconversion of ammonia and nitrite as ligands coordinated to ruthenium. In solutions of pH greater than 2, the oxidation of $[(tpy)(bpy)Ru(NH_3)]^{2+}$ is characterized by a broad wave whose peak potential (E_p^a = 0.89 V) is pH independent over the pH range 2–7 (Figure 1A). The oxidation is chemically irreversible, as shown by the absence of a rereduction wave and by the appearance of a wave characteristic of the nitrosyl product, $[(tpy)(bpy)Ru(NO)]^{3+}$, at $E_{1/2}$ = 0.23 V. It is important to realize that an acid–base equilibrium exists between the nitro and nitrosyl complexes

$$[(tpy)(bpy)Ru(NO)]^{3+} + H_2O \rightleftharpoons [(tpy)(bpy)Ru(NO_2)]^{+} + 2H^{+}$$

and that the two forms (nitro and nitrosyl) are present in equal concentrations in solutions at pH 2.3.[11]

In Table I are summarized reduction potential data for the series of Ru- and Os-based reversible couples of relevance in this study.

Bulk electrolysis of solutions containing $[(tpy)(bpy)Ru(NH_3)]^{2+}$ at pH >2 at an applied potential of 0.80 V occurs with n = 6 and the quantitative conversion of $[(tpy)(bpy)Ru(NH_3)]^{2+}$ to $[(tpy)(bpy)Ru(NO)]^{3+}$.[11] In acidic aqueous solution or in acetonitrile, $[(tpy)(bpy)Ru(NH_3)]^{2+}$ has a reversible Ru(III/II) wave (at $E_{1/2}$ = 1.04 (CH_3CN) or 0.93 (H_2O)) and can be oxidized quantitatively by one electron to $[(tpy)(bpy)Ru(NH_3)]^{3+}$.

The reverse reaction, the reduction of the corresponding nitrosyl complex, is shown in Figure 1B. The voltammogram in Figure 1B shows that in acidic solution $[(tpy)(bpy)Ru(NO)]^{3+}$ is reduced first by a reversible, one-electron process followed by an irreversible, multielectron process that leads to $[(tpy)(bpy)Ru(NH_3)]^{2+}$. Coulometry using applied potentials more negative than the second reduction wave in 0.1 M H_2SO_4 yields n = 5.99 ± 0.02 and $[(tpy)(bpy)Ru(NH_3)]^{2+}$ as the sole product. The identity of the product was verified by comparing the cyclic voltammogram and absorption spectra with an authentic sample.[11b]

Electrochemical Reduction of $[(tpy)(bpy)Ru(NO)]^{3+}$ in Acetonitrile. A cyclic voltammogram of $[(tpy)(bpy)Ru(NO)]^{3+}$ in acetonitrile is shown in Figure 2. In the voltammogram a chemically reversible reduction appears at $E_{1/2}$ = 0.45 V and a second reductive process at E_p^c = −0.25 V. In addition, oxidation waves can be seen that arise from the appearance of small amounts of products generated as a consequence of reduction past the second wave. In earlier work,[15,20] it was shown that the consequence of reduction at the first wave is a one-electron, largely ligand-localized process that is chemically reversible:

$$[(tpy)(bpy)Ru^{II}(NO^{+})]^{3+} + e^{-} \rightleftharpoons [(tpy)(bpy)Ru^{II}(NO)]^{2+}$$

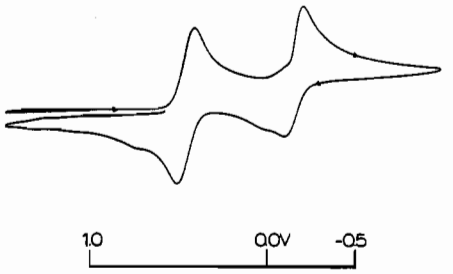

Figure 2. Cyclic voltammogram of $[(tpy)(bpy)Ru(NO)]^{3+}$ in acetonitrile with 0.1 M TEAP added as supporting electrolyte. The scan rate is 200 mV/s, and the working electrode is a Pt disk.

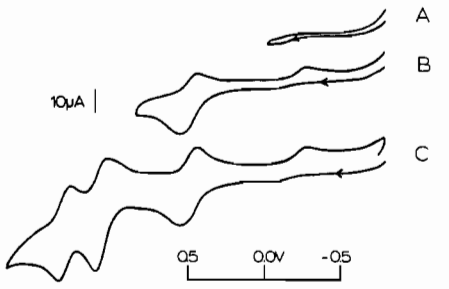

Figure 3. Cyclic voltammograms of the product of the reduction of $[(tpy)(bpy)Ru(NO)]^{3+}$ at −0.3 V. The solution is 0.1 M in TEAP in acetonitrile, the scan rate is 200 mV/s, and the working electrode is a Pt disk. See text for discussion.

The second wave is also a one-electron process that is probably ligand-localized as well but is chemically irreversible even in acetonitrile. As noted earlier,[20] electrochemical reduction of $[(tpy)(bpy)Ru(NO)]^{3+}$ past the first wave (at 0.30 V) results in a one-electron reduction (n = 1.00 ± 0.02 electrons) and no change in the cyclic voltammogram following reduction. However, reduction past the second wave occurs with n values of between 0.75 and 1.00 electron upon repeated trials and generates new products as determined by voltammetry.

A typical cyclic voltammogram of the products obtained following the second reduction of $[(tpy)(bpy)Ru(NO)]^{3+}$ in acetonitrile is shown in Figure 3C. The wave at $E_{1/2}$ = 1.30 V corresponds to the couple $[(tpy)(bpy)Ru(NCCH_3)]^{3+/2+}$. The product having E_p^a = 1.05 V is $[(tpy)(bpy)Ru(NO_2)]^{+}$, as evidenced both by the peak position and by the fact that oxidation at this wave produces $[(tpy)(bpy)Ru(NO_3)]^{+}$ and $[(tpy)(bpy)Ru(NO)]^{3+}$, which are known reaction products of the oxidation of $[(tpy)(bpy)Ru(NO_2)]^{+}$.[21] An additional wave appears at E_p^a = 0.53 V as a broad shoulder on the side of the oxidative wave for the $[(tpy)(bpy)Ru(NO)]^{3+}/[(tpy)(bpy)Ru(NO)]^{2+}$ couple. This wave has its origin in the reoxidation of an intermediate that is unstable and reverts quantitatively to $[(tpy)(bpy)Ru(NO)]^{3+}$ with n = 2.0 ± 0.2 following reoxidation at 0.60 V. The n value was inferred form the relative peak currents for the oxidation wave of the intermediate, the oxidation wave for $[(tpy)(bpy)Ru(NO_2)]^{+}$, and the charge passed on bulk oxidation past each of the two waves.

The E_p^a value for the intermediate is only slightly more positive than E_p^a for the $[(tpy)(bpy)Ru(NO)]^{3+/2+}$ couple. However, that it is present and upon oxidation gives the nitrosyl complex is illustrated in Figure 3. Note from the traces in Figure 3 that when oxidative scans are initiated at potentials more negative than the second nitrosyl-based reduction, no sign of the wave for the process $[(tpy)(bpy)Ru(NO^{-})]^{+} \rightarrow [(tpy)(bpy)Ru(NO\cdot)]^{2+} + e^{-}$ is observed. Reversal of the potential scan before reaching the oxidation

(19) Murphy, W. R., Jr. Ph.D. Dissertation, The University of North Carolina, 1984.
(20) Callahan, R. W.; Meyer, T. J. *Inorg. Chem.* **1977**, *16*, 574.
(21) Keene, F. R.; Salmon, D. J.; Walsh, J. L.; Abruna, H. D.; Meyer, T. J. *Inorg. Chem.* **1980**, *19*, 1896.

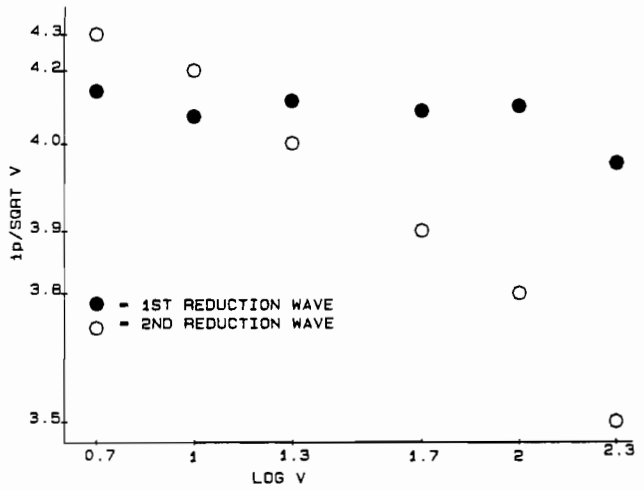

Figure 4. Plot of $i_p^c/v^{1/2}$ vs. log v for the first (closed circles) and second (open circles) reduction waves of $[(tpy)(bpy)Ru(NO)]^{3+}$ in acetonitrile (0.1 M TEAP).

wave of the intermediate shows that no nitrosyl complex is present in the solution (Figure 3A). The characteristic waves for the nitrosyl complex only appear following oxidative scans past E_p^a for the intermediate at 0.53 V (Figure 3B). The oxidation with $E_p^a = 0.53$ V appears to be ligand-localized because of its sensitivity to medium effects. Thus E_p^a shifts from 0.53 to 0.80 V when the electrolyte is changed from 0.1 M TEAP to 0.1 M TBAH. The species responsible for this oxidation is clearly an unstable intermediate, since, over a period of 20 min, it decomposes to give $[(tpy)(bpy)Ru(NO)]^{3+}$. This is evidenced by the growth of the wave at −0.25 V characteristic of the $[(tpy)(bpy)Ru(NO)]^{2+/+}$ reduction. We have been unable to isolate the intermediate, and attempts to trap it by the addition of possible scavengers have given inconclusive results.[19]

The scan rate dependence of the peak currents for the first and second reduction waves for $[(tpy)(bpy)Ru(NO)]^{3+}$ were obtained. The current functions, $i_p/v^{1/2}$, are shown plotted against log v in Figure 4[18] for both waves. For the first wave, the relative invariance of the current function with log v suggests that, up to 200 mV/s, any chemical reactions that occur before the charge-transfer step must be rapid on this time scale.[18b]

For the second reduction, the current function plotted against log v decreases with increasing scan rate, suggesting that there is a chemical reaction that precedes the charge-transfer step. The simplest explanation is that the second reduction is preceded by a chemical step that is slow on the cyclic voltammetry time scale, which in mechanistic form becomes[18b,22]

$$[(tpy)(bpy)Ru(NO\cdot)]^{2+} \underset{k_{-1}}{\overset{k_1}{\rightleftharpoons}} Ox \underset{-e^-}{\overset{+e^-}{\rightleftharpoons}} Red$$

or that the heterogeneous charge-transfer rate is slow:

$$[(tpy)(bpy)Ru(NO\cdot)]^{2+} + e^- \rightleftharpoons Red$$

If the former is correct, the charge-transfer step, $e^- + Ox \rightleftharpoons Red$, is probably reversible, since the current function for the second reduction is the same or slightly larger than the current function for the first at slow scan rates. If further redox steps occur past the initial charge-transfer step, an increase in the current function is expected.[18]

The chemical origins of the relatively slow second reduction may lie in significant structural changes in the complex possibly at the RuNO group. The RuNO link in $[(tpy)(bpy)Ru^{II}(NO)]^{3+}$ is, no doubt, linear and, given the electronic structures involved, is expected to be bent in the twice-reduced complex, $[(tpy)(bpy)Ru^{II}(NO)]^{+}$.[23,24] If the RuNO link in $[(tpy)(bpy)Ru^{II}(NO)]^{2+}$ is linear, a significant vibrational contribution from the

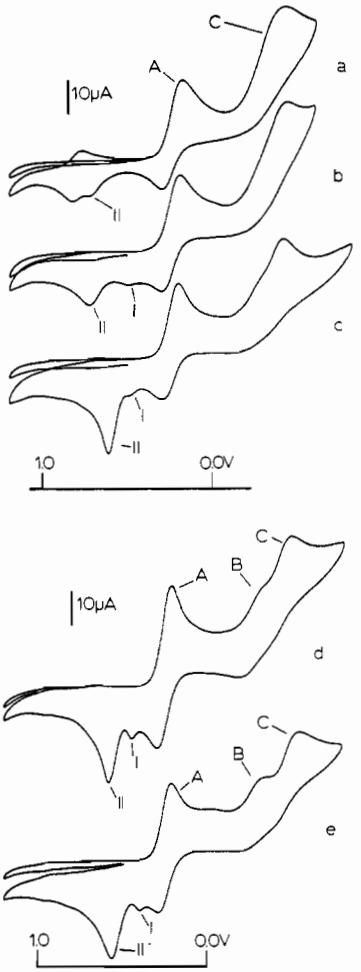

Figure 5. Cyclic voltammograms of $[(tpy)(bpy)Ru(NO)]^{3+}$ in aqueous solutions of varying pH: (a) pH 1.41; (b) pH 2.57; (c) pH 2.66; (d) pH 3.86; (e) pH 4.68. The scan rate is 100 mV/s, and the working electrode is carbon paste.

linear to bent interconversion could decrease heterogeneous and homogeneous electron-transfer rate constants. In the limit of a preequilibrium, the heterogeneous charge-transfer step would be preceded by interconversion between linear and relatively unstable, "bent" isomers of $[(tpy)(bpy)Ru(NO)]^{2+}$ with the bent isomer present in spectroscopically nondetectable amounts. A second, kinetically equivalent possibility suggested by a reviewer is that associated with the second reduction is the opening of a tpy chelate arm to give a five-coordinate intermediate (bpy-py is a ring opened tpy):

$$(tpy)(bpy)Ru(NO\cdot)^{2+} + e^- \rightarrow (bpy\text{-}py)(bpy)Ru(NO^-)^+$$

In this interpretation, the kinetic inhibition to the gain of the second electron would have its origin in the substitutional processes associated with the change in coordination number at the metal. Reduction of nitroprusside, $[Fe(CN)_5NO]^{2-}$, does occur with loss of a CN^- ligand.[25,29]

pH Dependence of the Reduction of $[(tpy)(bpy)Ru(NO)]^{3+}$. Since protons are involved in the net reduction of $[(tpy)(bpy)Ru(NO)]^{3+}$ to $[(tpy)(bpy)Ru(NH_3)]^{2+}$, the pH dependence of the electrochemical reduction of the nitrosyl complex was investigated in aqueous solution and some of the results obtained are illustrated in Figure 5. At pH 1.41 (Figure 5a) the two reduction waves of $[(tpy)(bpy)Ru(NO)]^{3+}$ are apparent and, following a reductive scan, the reversible wave for the $[(tpy)(bpy)Ru(NH_3)]^{3+/2+}$ couple also appears. However, a new oxidative wave appears at $E_p^a = 0.72$ V (wave II). As the pH is

(22) Reference 16, p 4455 ff.
(23) Masek, J. Fresenius' *Z. Anal. Chem.* **1967**, *224*, 99.
(24) McCleverty, J. A. *Chem. Rev.* **1979**, *79*, 53.
(25) Uchiyana, S.; Muto, G. *J. Electroanal. Chem. Interfacial Electrochem.* **1981**, *127*, 275.

increased to 2.57 (Figure 5b), the wave for $[(tpy)(bpy)Ru(NH_3)]^{2+}$ is no longer observable following the reductive scan and the second nitrosyl-based reduction (wave C) has shifted to a more negative potential. Also, note that following the reductive scan the peak current for wave II is increased and a new oxidation wave (wave I) appears at $E_p^a = 0.50$ V. At pH 2.66 (Figure 5c), the peak currents are increased for both I and II, following the reductive scan, and their peak potentials have shifted reductively. It should also be pointed out that, in the nitrosyl reduction region, a shoulder (wave B) appears on wave C and wave C has decreased in peak current. Further increases in pH, to 3.86 and 4.68 (Figure 5d,e), lead to reductive shifts in waves C and I, but waves II and B are pH independent. The peak current for wave I reaches a maximum around pH 4 and subsequently decreases as the pH is increased further.

The overall features and pH independence of waves A and B suggest that they are the same processes as observed in acetonitrile. At the higher pH values where the second (wave B) and third (wave C) reductions are well-separated, the ratios of the first and second reductive peak currents, $i_p^c(B)/i_p^c(A)$, can be evaluated and it is obvious that the ratio is less than 1. It follows by inference from the data in acetonitrile that the decrease in i_p^c for the second wave may also be a kinetic consequence of the structural change associated with the second reduction.

In acidic solution, the shift to more positive potentials of the third reduction (wave C) as acidity is increased causes wave C to overlap with wave B, which is pH-independent. The ratio of the total peak current for the combined waves B and C to the peak current of the first reduction, $i_p^c(B+C)/i_p^c(A)$, increases sharply when the pH is decreased from 2.66 to 2.57. The origin of this effect appears to lie in protonation of the doubly reduced intermediate in this pH range, $[(tpy)(bpy)Ru^{II}(NO^-)]^+ + H^+ \rightarrow [(tpy)(bpy)Ru(NHO)]^{2+}$, followed by further reduction at the electrode[25] to give the ammine product. The evidence favoring this interpretation is that the enhanced peak current ratio in acidic solution is also paralleled by the appearance, for the first time, of the ammine product following a reductive scan.

Further evidence for the existence of proton-dependent reactions comes from the pH-dependent properties of the new waves, I and II. These waves are apparently due to partially reduced intermediates, which can be intercepted by the reversal feature inherent in cyclic voltammetry. At pH 4.6, the second and third reductions are well-separated, and potentiostating a solution containing $[(tpy)(bpy)Ru(NO)]^{3+}$ at −0.30 V generates only the intermediate oxidized at wave I to a significant degree (Figure 6, part 1). Wave I is itself pH-dependent, and a plot of the oxidative peak potential for the wave, $E_p^a(I)$, against pH is shown in Figure 7. The line shown has a slope of 26 mV/pH unit, consistent with a two-electron oxidation with loss of one proton. The unusually large scatter in the data may be due to the chemical and/or charge-transfer irreversibility of the oxidation process. The chemical composition and certain details of the formation of intermediate I can be deduced from the available data. The intermediate appears as a consequence of a two-electron, pH-independent reduction of $[(tpy)(bpy)Ru^{II}(NO)]^{3+}$ through waves A and B. Once formed, the intermediate can be oxidized in a two-electron step with the loss of a proton to return to the starting nitrosyl complex. From this information, it appears that the intermediate has the composition $[(tpy)(bpy)Ru(NHO)]^{2+}$ and is formed by the addition of a proton to $[(tpy)(bpy)Ru(NO^-)]^+$ following the addition of a second electron:

$$[(tpy)(bpy)Ru^{II}(NO\cdot)]^{2+} \xrightarrow{+e^-} [(tpy)(bpy)Ru^{II}(NO^-)]^+$$

$$[(tpy)(bpy)Ru^{II}(NO^-)]^+ \xrightarrow{+H^+} [(tpy)(bpy)Ru^{II}(NHO)]^{2+}$$

In the oxidation at wave I both a proton and two electrons must be lost in a rapid net process from $[(tpy)(bpy)Ru(NHO)]^{2+}$ to return to $[(tpy)(bpy)Ru(NO)]^{3+}$.

The intermediate signaled by the appearance of wave II appears to result from reduction at wave C. This point is made in part 2 of Figure 6, where a large enhancement in wave II occurs when the potential of the electrode is held past wave C. It is also notable

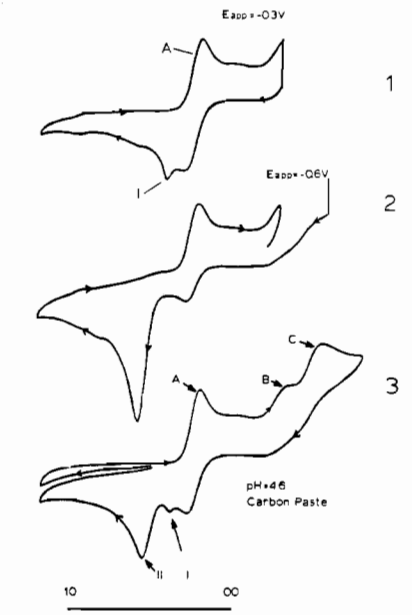

Figure 6. Potential dependence of the partially reduced intermediates found in the reduction of $[(tpy)(bpy)Ru(NO)]^{3+}$: (1) holding potential −0.30 V; (2) holding potential −0.6 V; (3) potential sweep from +0.50 to +1.20 to −1.00 to +1.20 to +0.50 V. The solution pH is 4.68, the working electrode is carbon paste, and the scan rate is 100 mV/s.

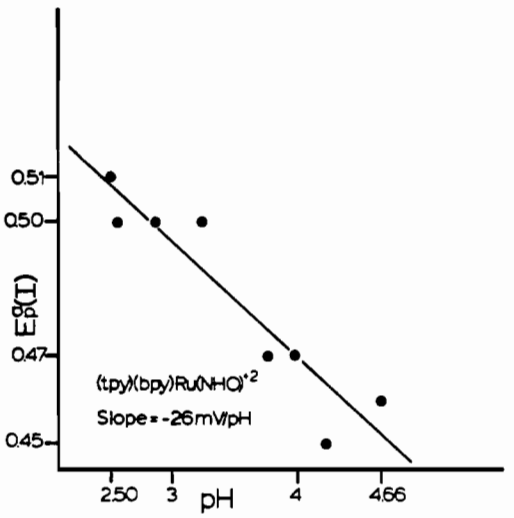

Figure 7. Plot of E_p^a for wave I of $[(tpy)(bpy)Ru(NO)]^{3+}$ against solution pH. The correlation coefficient is 0.93.

that the intermediate associated with wave II grows at the expense of the intermediate associated with wave I and, therefore, that I is a precursor of II.

The pH dependence of the peak potential for wave C is shown in Figure 8. The line has a slope of −71 mV/pH unit, which corresponds most nearly to the −59 mV/pH unit slope expected for a one proton per electron reduction. At higher pH values, waves B and C are well separated and have roughly the same integrated areas, showing that the reduction at wave C is also a one-electron process. Since reduction at wave C produces II at the expense of $[(tpy)(bpy)Ru(NHO)]^{2+}$, at wave C, a one-electron, one-proton reduction of $[(tpy)(bpy)Ru(NHO)]^{2+}$ must occur to give either a Ru^V–nitrido intermediate or its corresponding hydrate:

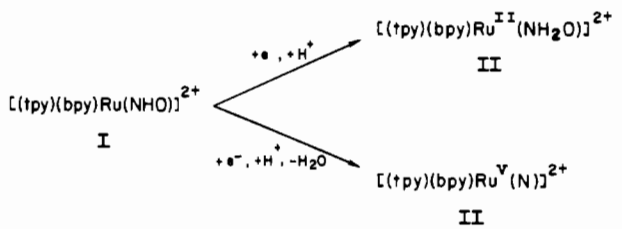

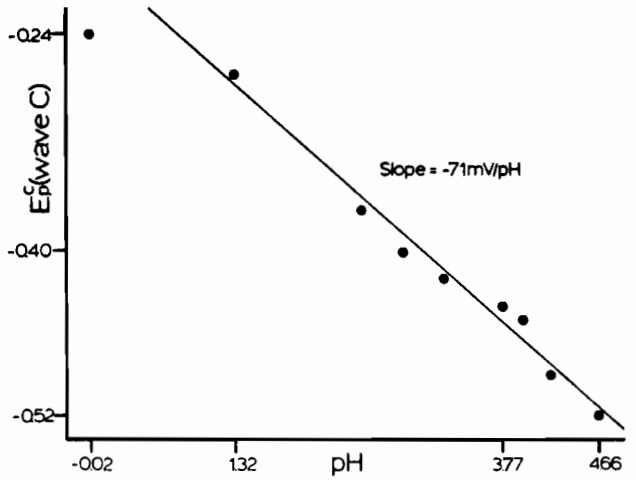

Figure 8. Plot of E_p^c for wave C of $[(tpy)(bpy)Ru(NO)]^{3+}$ against solution pH. The correlation coefficient is 0.99. Note that the point at pH −0.02 and $E_p^c(C) = -0.24$ V was not included in the data analysis.

The suitability of oxidation-state descriptions for such intermediates will be discussed in a later section.

At wave II oxidation of $[(tpy)(bpy)Ru(N)]^{2+}$ or $[(tpy)(bpy)Ru(NH_2O)]^{2+}$ occurs, in the net sense, to give back the nitrosyl complex, $[(tpy)(bpy)Ru(NO)]^{3+}$. Above pH 3, the oxidation process is pH-independent, suggesting an initial oxidation to $[(tpy)(bpy)Ru(N)]^{3+}$ or $[(tpy)(bpy)Ru(NH_2O)]^{3+}$, followed by an electron–proton-loss step or steps to give the nitrosyl complex. Below pH 3 a dramatic shift in E_p^a for wave II occurs from 0.58 to 0.70 V, suggesting that in acidic solution oxidation involves a protonated species, perhaps $[(tpy)(bpy)Ru(NH)]^{3+}$ or the protonated hydrate $[(tpy)(bpy)Ru(NH_2OH)]^{3+}$. It is also notable that in acidic solution the ammine product $[(tpy)(bpy)Ru(NH_3)]^{2+}$ begins to appear in competition with II following a reductive scan through wave C. Presumably, this signals a further proton-dependent reduction of $[(tpy)(bpy)Ru(NH)]^{3+}$ or $[(tpy)(bpy)Ru(NH_2OH)]^{3+}$ on the cyclic voltammetry time scale.

Intermediate II cannot be prepared in the net sense by electrochemical reduction. Partial coulometric reduction of $[(tpy)(bpy)Ru(NO)]^{3+}$ at pH 4 past wave C leads to the buildup of II as shown by the appearance of wave II. However, the intermediate is pseudostable under these conditions. Further reduction gives only $[(tpy)(bpy)Ru(NH_3)]^{2+}$ and on standing only the ammine and nitrosyl complexes are observed in solution. The nitro complex $[(tpy)(bpy)Ru(NO_2)]^{+}$ slowly appears in these solutions as a consequence of the acid–base interconversion:

$$[(tpy)(bpy)Ru(NO)]^{3+} + H_2O \rightarrow [(tpy)(bpy)Ru(NO_2)]^{+} + 2H^{+}$$

Recall that from the measured equilibrium constant for the acid–base interconversion, the nitro and nitrosyl complexes are present in equal amounts at pH 2.3 when the system reaches acid–base equilibrium.[11b,15] The electrochemical experiments are only possible above pH 2.3 because nitrosyl → nitro interconversion is slow.

Oxidation of $[(tpy)(bpy)Os(NH_3)]^{2+}$. In acidic solution, the voltammetric behavior of $[(tpy)(bpy)Os(NH_3)]^{2+}$ is analogous to that for $[(tpy)(bpy)Ru(NH_3)]^{2+}$ in that a single wave is observed for the Os(III/II) couple, although the M(III/II) reduction potential is shifted from 0.78 V (M = Ru) to 0.41 V for Os (Figure 10). The oxidation of $[(tpy)(bpy)Os(NH_3)]^{2+}$ to $[(tpy)(bpy)Os(NH_3)]^{3+}$ is chemically reversible from pH 1.66 to 4.52. However, by pH 6.80, the oxidation process is chemically irreversible and two waves appear in the cyclic voltammogram during an oxidative scan. Figure 10 shows a better view of the voltammogram of $(tpy)(bpy)Os(NH_3)^{2+}$ at pH 6.8. One wave appears at $E_p^a = 0.45$ V due to the oxidative component of the pH-independent Os(II)/Os(III) couple, $[(tpy)(bpy)Os(NH_3)]^{2+/3+}$, and a second wave appears at $E_p^a = 0.55$ V. Increasing the scan rate to 1 V/s results in the loss of the oxidative wave at 0.55 V, and

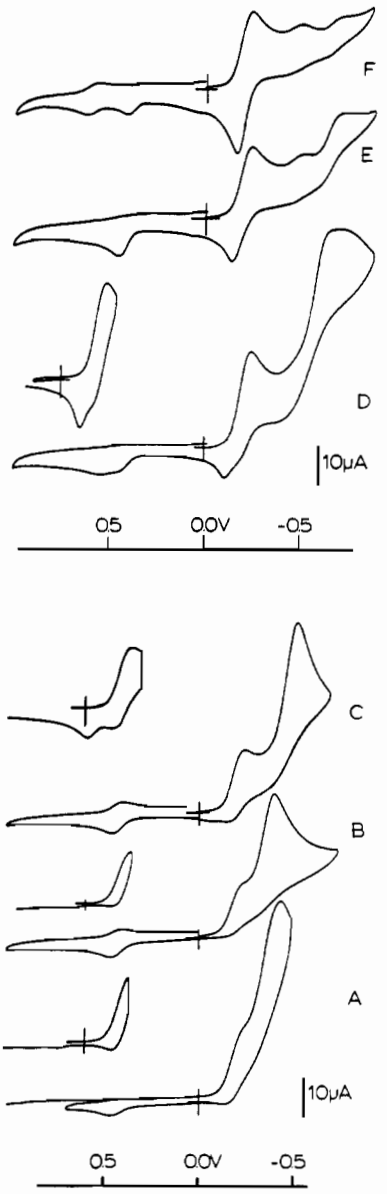

Figure 9. Cyclic voltammograms of $[(tpy)(bpy)Os(NO)]^{3+}$ in solutions of varying pH: (A) pH 1.66; (B) pH 2.96; (C) pH 4.52; (D) pH 6.80; (E) 8.18; (F) pH 9.15. The scan rate is 100 mV/s, and the working electrode is glassy carbon. The voltammograms offset to the left of each voltammogram show the effect of switching the direction of the potential scan just past the first reduction wave. The cross marks 0.00 V, and the potential scan is the same as for the standard voltammograms.

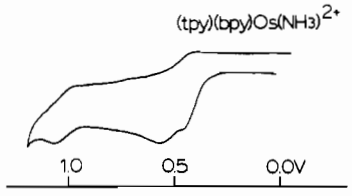

Figure 10. Cyclic voltammogram of $[(tpy)(bpy)Os(NH_3)]^{2+}$ at pH 6.8. The working electrode is carbon paste, and the scan rate is 100 mV/s.

a reductive component of the oxidation wave at 0.45 V appears. These data provide clear evidence for an additional one-electron-oxidation step past the Os(II) → Os(III) + e^- stage. The most straightforward interpretation of the results is that, by pH 6.80, rate-determining loss of a proton or protons occurs from $[(tpy)(bpy)Os(NH_3)]^{3+}$

$$[(tpy)(bpy)Os^{III}(NH_3)]^{3+} \xrightarrow{-H^+} [(tpy)(bpy)Os^{III}(NH_2)]^{2+}$$

followed by oxidation of Os(III) to Os(IV)

$$[(tpy)(bpy)Os^{III}(NH_2)]^{2+} \xrightarrow[E_p^a = 0.55\ V]{-e^-,\ -H^+} [(tpy)(bpy)Os^{IV}(NH)]^{2+}$$

We have no direct evidence for the nature of the two-electron-oxidation product but the suggestion of an Os(IV)–imido complex is reasonable, given the evidence obtained earlier for the Ru analogue, $[(tpy)(bpy)Ru^{IV}(NH)]^{2+}$.[11] Oxidation past +0.55 V showed a new wave at −0.2 V consistent with the formation of some nitrosyl complex in a reaction analogous to the oxidation of $[(tpy)(bpy)Ru^{II}(NH_3)]^{2+}$. In addition, scanning to more anodic potentials showed a new pair of waves with $E_{1/2} \approx +1.05$ V (Figure 10). Repeated scans at different sweep rates suggested this redox process was linked to the appearance of the wave at $E_p^a = 0.55$ V, suggesting the formation of a further product derived from $[(tpy)(bpy)Os^{IV}(NH)]^{2+}$. This chemistry is under continuing investigation, but present studies indicate that this new species is not an intermediate in the oxidation of coordinated amine to nitrosyl.

In the pH region 1.66–4.52, E_p^a for the $Os^{III}(NH_3)/Os^{II}(NH_3)$ couple is pH-independent, suggesting that the dominant form of the Os(III) complex once generated is the ammine and hence that the pK_a value for proton loss from $[(tpy)(bpy)Os(NH_3)]^{3+}$ is greater than or near 6.8.

Because the $[(tpy)(bpy)Os^{III}(NH_3)]^{3+}/[(tpy)(bpy)Os^{II}(NH_3)]^{2+}$ couple is proton independent while the $[(tpy)(bpy)Os^{IV}(NH)]^{2+}/[(tpy)(bpy)Os^{III}(NH_2)]^{2+}$ couple is proton dependent, by pH 8.18, the potential for the IV/III couple has overtaken the potential for the III/II couple and the initial oxidation becomes multielectron in nature. For the related Ru complex, even at pH 3.97 only a multielectron wave is observed, showing that E_p^a for an analogous Ru(IV)/Ru(III) couple, $[(tpy)(bpy)Ru^{IV}(NH)]^{2+}/[(tpy)(bpy)Ru^{III}(NH_2)]^{2+}$, occurs at a more reductive potential than E_p^a for the Ru(III)/Ru(II) couple, $[(tpy)(bpy)Ru(NH_3)]^{3+/2+}$. Hence, under these conditions the Ru(III) complex is unstable with respect to disproportionation:

$$2[(tpy)(bpy)Ru^{III}(NH_3)]^{3+} \xrightarrow{-2H^+} 2[(tpy)(bpy)Ru^{III}(NH_2)]^{3+} \rightarrow [(tpy)(bpy)Ru^{IV}(NH)]^{2+} + [(tpy)(bpy)Ru^{II}(NH_3)]^{2+}$$

It was this fact that was taken advantage of in an earlier study to generate solutions containing $[(tpy)(bpy)Ru^{IV}{=}NH]^{2+}$ with use of rapid-mixing techniques.[11] The same type of observation was made earlier by Taube and Rudd, who reported that disproportionation of $Ru(NH_3)_5(py)^{3+}$ (py = pyridine) occurs in basic solution.[26]

Because of the implied difference in pH dependences between the Ru(III)/Ru(II) and Ru(IV)/Ru(III) couples, in more acidic solutions it is conceivable that the potential for the Ru(IV)/Ru(III) couple could cross over that of the Ru(III)/Ru(II) couple, which would lead to separated Ru(II) → Ru(III) and Ru(III) → Ru(IV) processes as found for the Os complex at pH 6.8. However, it is impossible to explore this point experimentally, because in acidic solutions the concentration of the kinetically important amido complex is too low and further oxidation of Ru(III) is too slow to observe experimentally.

It is notable that on the oxidation side there is no evidence for the appearance of additional intermediates past the initial M(II) $\xrightarrow{-e^-}$ M(III) $\xrightarrow{-e^-}$ M(IV) stage. Notice from Figure 5 that this is an expected result. Further oxidation, no doubt, occurs through intermediates II, $[(tpy)(bpy)Ru(N)]^{2+}$ or $[(tpy)(bpy)Ru(NH_2O)]^{2+}$, and I, $[(tpy)(bpy)Ru(NHO)]^{2+}$. However, they can not build up as intermediates because, once formed, they are themselves oxidized at potentials less positive than the potentials for oxidation of M(II) to M(III). As a consequence, the wave corresponding to the M(II) → M(III) → M(IV) step is multielectron in character and results in the direct oxidation of bound NH_3 to NO. The multielectron character of the oxidation wave is illustrated graphically in Figure 1 at pH 3.97 by comparing integrated peak areas for the oxidation process with the return wave for nitrosyl reduction, which (see above) involves the one-electron reduction of $[(tpy)(bpy)Ru(NO)]^{3+}$ to $[(tpy)(bpy)Ru(NO)]^{2+}$.

In comparisons of the Ru and Os systems with regard to the potentials for the M(IV)/M(III) and M(III)/M(II) couples, some interesting conclusions can be drawn. As noted above, in pH ranges where the Os(IV)/Os(III) couple is discernible, the Ru(IV)/Ru(III) couple is not. Thus, it would appear that, as for intermediates I and II, further oxidation of Ru(III) occurs at potentials less positive than that of the Ru(II) → Ru(III) oxidation. By inference, Os(III) is relatively a more stable oxidation state than Ru(III) in this coordination environment. As shown by the redox potential data (vs. SSCE, 25 °C, pH 7[27]), the same situation exists for the related oxo/aquo couples:

$$[(tpy)(bpy)Ru{=}O]^{2+} \xrightarrow{0.62\ V} [(tpy)(bpy)Ru{-}OH]^{2+} \xrightarrow{0.49\ V} [(tpy)(bpy)Ru{-}OH_2]^{2+}$$

$$[(tpy)(bpy)Os{=}O]^{2+} \xrightarrow{0.42\ V} [(tpy)(bpy)Os{-}OH]^{2+} \xrightarrow{0.09\ V} [(tpy)(bpy)Os{-}OH_2]^{2+}$$

Notice from the redox potential data that, in the aquo system, $[(tpy)(bpy)Ru^{III}(OH)]^{2+}$ is stable toward disproportionation but only by ~130 mV while $[(tpy)(bpy)Os^{III}(OH)]^{2+}$ is stable toward disproportionation by 330 mV.

Ironically, it has been concluded that in the related diaquo/dioxo systems $[(bpy)_2M^{VI}(O)_2]^{2+}/[(bpy)_2M^{IV}(O)(OH_2)]^{2+}/[(bpy)_2M^{III}(OH)(OH_2)]^{2+}/[(bpy)_2M^{II}(OH_2)_2]^{2+}$ the origin of the relative stability of Os(III) compared to that of Ru(III) lies in the relative instability of Os(IV) compared to Ru(IV).[27]

In comparisons of the ammine and aquo systems (vs. SSCE, 25 °C, pH 6.86), e.g.

$$[(tpy)(bpy)Os(NH)]^{2+} \xrightarrow{E_p^a = 0.55\ V} [(tpy)(bpy)Os(NH_2)]^{2+} \xrightarrow{0.45\ V} [(tpy)(bpy)Os(NH_3)]^{2+}$$

perhaps the most important factors that distinguish their behavior are (1) the relatively low acidity of the $[(tpy)(bpy)M(NH_3)]^{3+}$ ions, which has an important impact on the relative potentials for the M(IV)/M(III) and M(III)/M(II) couples and (2) the relative instability of the M(IV)–imido complex relative to the M(IV)–oxo complexes toward further reactions such as "hydration"[11]

$$[(tpy)(bpy)Ru^{IV}{=}NH]^{2+} + H_2O \rightarrow [(tpy)(bpy)Ru^{II}(NH_2OH)]^{2+}$$

or further oxidation.

Reduction of $[(tpy)(bpy)Os(NO)](PF_6)_3$. In acetonitrile, two reversible reduction waves appear for $[(tpy)(bpy)Os(NO)]^{3+}$ at $E_{1/2} = -0.02$ and −0.24 V. The first reduction is ligand-localized and chemically reversible, but the second reduction leads to products similar to those described above for the Ru complex. Both reductions are one-electron processes.

In discussing the pH dependence of the reduction of the Os–NO complex in water, it is convenient to begin by discussing the results obtained in slightly basic solutions. As shown in Figure 9F,E, at pH 9.15 and 8.18, respectively, the pattern of waves is similar to the pattern observed for the related Ru complex at pH 4.7. The decrease in peak currents for the second and third reduction waves is, once again, a consequence of the structurally induced, slow $Os^{II}(NO\cdot) + e^- \rightarrow Os^{II}(NO^-)$ reduction. If the structural change involves a linear to bent change in Os–NO, the wave at $E_p^c = -0.50$ V would correspond to a further reduction to give the bent isomer:

$$[(tpy)(bpy)Os^{II}(NO\cdot)]^{2+} \xrightarrow{+e^-} [(tpy)(bpy)Os^{II}(NO^-)]^{+}$$

If it involves loss of a tpy arm, the second reduction would be

$$[(tpy)(bpy)Os^{II}(NO\cdot)]^{2+} \xrightarrow{+e^-} [(bpy\text{-}py)(bpy)Os(NO)]^{+}$$

(26) Rudd, D. P.; Taube, H. *Inorg. Chem.* **1971**, *10*, 1543.

(27) Takeuchi, K. J.; Thompson, M. S.; Pipes, D. W.; Meyer, T. J. *Inorg. Chem.* **1984**, *23*, 1845.

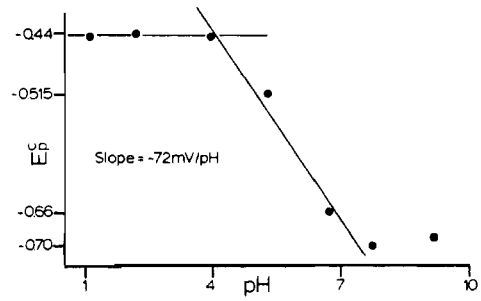

Figure 11. Plot of E_p^c for the most negative reduction wave for $[(tpy)(bpy)Os(NO)]^{3+}$ ($[(tpy)(bpy)Os(NO)]^{2+} + ne^- + mH^+ \rightarrow$ reduced products) against solution pH. The correlation coefficient for the line with slope −72 mV/pH unit is 0.99.

The small wave at $E_{1/2} = 0.60$ V at pH 9.15 is attributable to the $[(tpy)(bpy)Os(NO_2)]^{2+/+}$ couple arising from slow nitrosyl → nitro interconversion:

$$[(tpy)(bpy)Os(NO)]^{3+} + 2OH^- \rightarrow [(tpy)(bpy)Os(NO_2)]^+ + H_2O$$

In the pH range 8.18–9.15, neither the second nor the third reduction process at $E_p^c = -0.50$ and −0.70 V is pH dependent. However, by pH 6.80 E_p^c for the second wave has shifted to $E_p^c = -0.66$ V, while the peak potential for the third wave remains unchanged. By inference, we presume that by pH 6.80 the proton concentration is sufficiently high that a new, relatively facile, proton-induced path appears for the second reduction:

$$[(tpy)(bpy)Os(NO\cdot)]^{2+} + H^+ \xrightarrow{+e^-} [(tpy)(bpy)Os(NHO)]^{2+}$$

The increase in peak current for the process at $E_p^c = -0.66$ V suggests that the proton-induced pathway is relatively more facile than the acid-independent pathway. The role of the added proton may be to assist in the linear to bent change at the nitrosyl ligand or to capture a trpy arm once opened.

It is notable that, following a reductive scan past the first reduction of the nitrosyl ligand at pH 6.80, a new oxidative wave appears for the first time at $E_p^a = -0.11$ V. The situation here is closely related to the results obtained for the intermediate formulated as I, $[(tpy)(bpy)Ru(NHO)]^{2+}$, and by analogy the oxidative wave at $E_p^a = -0.11$ V arises from oxidation of $[(tpy)(bpy)Os(NHO)]^{2+}$ to $[(tpy)(bpy)Os(NO)]^{3+}$.

Two features of the reoxidation of this intermediate are notable. The first is that, as for $[(tpy)(bpy)Ru(NHO)]^{2+}$, the reoxidation process is pH-dependent, at least in the pH region 4.52–8.18, where E_p^a shifts from −0.015 to −0.13 V. Above pH 8.18, the reoxidation overlaps with the reoxidative component of the first nitrosyl wave at $E_p^a = -0.16$ V. At pH 2.96 and below, the wave for the oxidation of intermediate I for Os has disappeared. In acidic solution, I does not build up but, rather, undergoes further reduction. I(Os) is observed most clearly at pH 6.80, where the second reduction is kinetically facile but the third reduction is not. However, by pH 4.52, the current associated with the third reduction is strongly enhanced and its E_p^c value has shifted sufficiently positively that it has overtaken the second reduction. Under these conditions I(Os) does not build up in solution but undergoes further reduction. Note from Figure 5 that the same situation exists for $[(tpy)(bpy)Ru(NHO)]^{2+}$ in the pH range 2.66–1.41.

The third reduction must also have a proton-dependent pathway (or pathways). The dependence of E_p^c on pH for the third wave is shown in Figure 11. From pH 9.15 to 6.80, the peak potential for the third reduction remains constant at −0.73 V. However, by pH 4.52 (Figure 9C) the peak potential for the third wave has shifted dramtically to more positive potentials up to or past E_p^c for the second wave. The shift in potential and increase in peak currents suggest the following: (1) By pH 4.52 a proton-induced pathway has appeared for the third reduction. (2) Since the third wave has overtaken the second, the proton dependence associated with the third wave must be of higher order than the first-order dependence found for the second wave for Ru. Since the third wave overtakes the second in acidic solution, only a single, multielectron reduction wave is observed with no buildup of the intermediate.

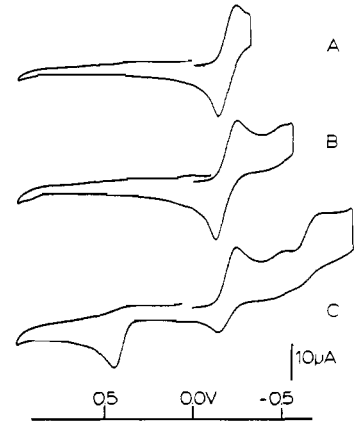

Figure 12. Potential dependence of the partially reduced intermediates formed in the reduction of $[(tpy)(bpy)Os(NO)]^{3+}$: (A) holding potential −0.33 V; (B) holding potential −0.56 V; (C) holding potential −0.92 V. The solution pH is 8.18, the working electrode is glassy carbon, and the scan rate is 100 mV/s. The scan was initiated in the negative direction, and the potential was held and then scanned positively.

In more acidic solutions, the trend continues and a single reductive peak potential is observed at $E_p^c = -0.39$ V at pH 2.96, while by pH 1.66, the same pattern of waves occurs although it is somewhat obscured by an increasingly significant reductive background. Note that reductive scans through the multielectron reduction wave at pH 4.52, 2.96, or 1.66 lead to the appearance of a chemically reversible wave at $E_{1/2} = 0.41$ V for the $[(tpy)(bpy)Os(NH_3)]^{3+/2+}$ couple without the appearance of intermediates.

By inference, in acidic solution, reduction of this complex at potentials cathodic of the third wave facilitates a net five-electron transfer (as judged by comparing the peak current for the third wave with that for the $[(tpy)(bpy)Os(NH_3)]^{3+/2+}$ couple, seen in Figure 9) to give $[(tpy)(bpy)Os^{II}(NH_3)]^{2+}$.

In order to search for intermediates at pH 8.18 and 9.15, where the three reductive waves are well separated, the scan potential was held past each wave in turn. Examples of the voltammograms obtained by this procedure are shown in Figure 12 for pH 8.18. In solutions at pH 8.18, reduction past the first wave is followed by reoxidation of the singly reduced nitrosyl complex, as expected (Figure 12A).

When the potential is held past the second reduction wave, a small broad wave is observed at ca. 0.05 V (Figure 12B) but the ratio ip^c/ip^a for the $[(tpy)(bpy)Os(NO)]^{3+/2+}$ reduction is 0.96. This result shows that reduction even past the second wave is chemically reversible and that, at pH 8.15, protonation of $[(tpy)(bpy)Os^{II}(NO^-)]^+$ to give $[(tpy)(bpy)Os(NHO)]^{2+}$ is slow on the time scale of the potential-hold experiment (seconds).

When the potential is held past the third wave (Figure 12C), the reoxidation waves for the $[(tpy)(bpy)Os(NO)]^{3+/2+}$ and $[(tpy)(bpy)Os(NO)]^{2+/+}$ couples are greatly diminished and the chemically irreversible oxidation wave at $E_p^a = 0.41$ V for the $[(tpy)(bpy)Os(NH_3)]^{3+/2+}$ couple appears. From the potential-hold experiments at pH 8.15 the following can be concluded: (1) Protonation of $[(tpy)(bpy)Os^{II}(NO^-)]^+$ is relatively slow. Once the third electron has been added, rapid formation of the ammine product occurs without the significant buildup of an intermediate or intermediates. (2) The *six*-electron product $[(tpy)(bpy)Os(NH_3)]^{2+}$ appears following the addition of only a third electron. And yet, from peak height comparisons in Figure 12, the first and third reduction waves appear to involve the same number of electrons and there is no evidence for a multiple-electron addition at the third wave, at least on the cyclic voltammetry time scale. (3) The continued appearance of the reoxidation wave for the process

$$[(tpy)(bpy)Os(NO\cdot)]^{2+} \xrightarrow{-e^-} [(tpy)(bpy)Os(NO^+)]^{3+}$$

under conditions where the ammine product appears without potential holding is probably a consequence of the slowness of the reduction at the second stage:

$$[(tpy)(bpy)Os(NO\cdot)]^{2+} \xrightarrow{+e^-} [(tpy)(bpy)Os(NO^-)]^+$$

Because of the slowness of the second step, not all of the singly reduced species will reach the third reduction stage on the time scale of the experiment and be recaptured by reoxidation to the starting nitrosyl:

$$[(tpy)(bpy)Os(NO\cdot)]^{2+} \xrightarrow{-e^-} [(tpy)(bpy)Os(NO^+)]^{3+}$$

(4) In the potential-hold experiment, the time scale for reduction is relatively much longer, and complete electrolysis occurs in the solution layers surrounding the electrode surface. Under these conditions, all of the singly reduced complex should be completely reduced to the three-electron stage

$$[(tpy)(bpy)Os(NO\cdot)]^{2+} \xrightarrow{+e^-} [(tpy)(bpy)Os(NO)]^+ \xrightarrow{+e^-} [(tpy)(bpy)Os(NO)]^0$$

and yet upon scan reversal there is still only a relatively small component for the reoxidation of $[(tpy)(bpy)Os(NO)]^{2+}$. The peak currents for the first nitrosyl reduction at $E_p^c = -0.26$ V and the irreversible ammine oxidation at $E_p^a = 0.41$ V are roughly the same. However, under these conditions the ammine oxidation is a two-electron process, suggesting that only part of the reduced complex reaches the ammine stage. It is possible to reconcile these observations—the continued appearance of the reoxidation of $[(tpy)(bpy)Os(NO\cdot)]^{2+}$ and the fact that an apparent three-electron reduction leads to a six-electron product—by invoking a disproportionation following the three-electron-reduction stage. There is precedence for disproportionation of intermediate oxidation states in related metal–oxo chemistry. For example, in acidic solution $[(tpy)Os^{VI}(O)_2(OH_2)]^{2+}$ undergoes a $3e^-/4H^+$ reduction to give $[(tpy)Os^{III}(H_2O)_3]^{3+}$ because of the instability with respect to disproportionation of the intermediate oxidation states Os(IV) and Os(V).[28] From the cyclic voltammetry results, further electrochemical reduction past the three-electron stage is slow, apparently creating a time window for disproportionation to occur:

$$2[(tpy)(bpy)Os(NO)]^0 + 3H_2O \rightarrow [(tpy)(bpy)Os(NH_3)]^{2+} + 3OH^- + [(tpy)(bpy)Os(NO)]^{3+}$$

$$[(tpy)(bpy)Os(NO)]^{3+} \xrightarrow[\text{rapid}]{+3e^-} [(tpy)(bpy)Os(NO)]^0$$

(5) Similar results were obtained at pH 9.15.

By contrast, in acidic solution below pH 4.52 (Figure 9A–C) large reductive peak currents signal the onset of multiple-electron-transfer processes. Potential scans through this region lead to the ammine product without the appearance of intermediates or of the reoxidation of $[(tpy)(bpy)Os(NO\cdot)]^{2+}$.

Reduction of Related Complexes. The electrochemical reductions of $[(tpy)(bpy)Os(NO)]^{3+}$ and $[(tpy)(bpy)Ru(NO)]^{3+}$, which were elaborated on here in detail, were shown to occur quantitatively ($n = 6.0 \pm 0.1$) by coulometry and product identification based on known $E_{1/2}$ values. In fact, chemical reduction using analgamated zinc in acidic solution and electrochemical reduction provide convenient synthetic routes to the corresponding ammine complexes. We have shown that the following reactions occur quantitatively by electrochemical or chemical reduction based on electrochemical monitoring of the products:

$$[(bpy)_2(py)Ru(NO)]^{3+} \xrightarrow{6e^-,\ 5H^+} [(bpy)_2(py)Ru(NH_3)]^{2+} + H_2O$$

$$E_{1/2}\{[(bpy)_2(py)Ru(NH_3)]^{3+/2+}\} = 0.82 \text{ V}$$

$$[(bpy)_2ClRu(NO)]^{2+} \xrightarrow{6e^-,\ 5H^+} [(bpy)_2(H_2O)Ru(NH_3)]^{2+} + Cl^-$$

$$E_{1/2}\{[(bpy)_2(H_2O)Ru(NH_3)]^{3+/2+}\} = 0.58 \text{ V}$$

$$[(bpy)_2Ru(NO_2)(NO)]^{2+} \xrightarrow{+12e^-,\ 10H^+} [(bpy)_2Ru(NH_3)_2]^{2+} + 2H_2O$$

$$E_{1/2}\{[(bpy)_2Ru(NH_3)_2]^{3+/2+}\} = 0.63 \text{ V (0.2 M } H_2SO_4)$$

General Discussion

In order to discuss our results on the interconversion of the nitro and ammine ligands, it is of value to consider the various stages involved before attempting to develop a coherent mechanism.

Nitro/Nitrosyl Interconversion. The reduction of free nitrite ion to ammonia proceeds through NO^+, which results from the acid–base equilibrium[23]

$$NO_2^- + 2H^+ \rightleftharpoons NO^+ + H_2O$$

and proceeds at appreciable rates in concentrated (8 M) acid. Similarly, the reactive form of the nitro ligand is the nitrosyl group. For polypyridyl complexes of Ru and Os,[12,15] and notably for the nitroprusside ion, $[(CN)_5Fe(NO)]^{2-}$,[25,29] the nitro and nitrosyl complexes are interrelated by acid–base equilibria:

$$[(tpy)(bpy)M(NO)]^{3+} + H_2O \rightleftharpoons [(tpy)(bpy)M(NO_2)]^+ + 2H^+$$

For the tpy–bpy complexes of Ru and Os, the pH values at which the two forms are present in equal amounts are 2.3 (M = Ru) and 8.6 (M = Os). The rates of the interconversion are dependent on the concentrations of acid or base, and thus at intermediate pH values, the equilibria are established slowly.[15,21] For $[(tpy)(bpy)Ru(NO)]^{3+}$, the conversion to the nitro form is slow even in a solution 3 pH units more basic than pH 2.3, which allowed us to investigate the pH dependence for the reduction of the complex over a relatively broad pH range. However, it should be realized that the pH-dependence studies described here are ultimately limited pH-wise by conversion to the reductively inactive nitro form as the pH is raised.

Nitrosyl Reduction. Stage 1. In the nitrosyl complexes $[(tpy)(bpy)M(NO)]^{3+}$, there are relatively low-lying levels largely $\pi^*(NO)$ in character, which provide a site for initial reduction.[15,20] In fact, the NO^+ ion is a relatively strong oxidant, which is readily reduced to nitric oxide.[15,28] Initial studies on nitrosyl reductions were based on the nitroprusside ion, which is reduced by an initial one-electron process to yield $[(CN)_5Fe(NO)]^{3-}$.[23,28] This species readily loses cyanide to form $[(CN)_4Fe(NO)]^{2-}$.

For polypyridyl complexes of Ru or Os of the type $[(tpy)(bpy)M(NO)]^{3+}$ (M = Ru, Os), a well-defined, reversible one-electron reduction occurs in acetonitrile, at $\pi^*(NO)$[15,20]

$$[(tpy)(bpy)M(NO^+)]^{3+} + e^- \rightleftharpoons [(tpy)(bpy)M(NO\cdot)]^{2+}$$

The reduction potential for the initial step is sensitive to the degree of $d\pi \rightarrow p\pi^*$ back-bonding between the metal and the NO group.[15] For example, systematic variations occur in $E_{1/2}$ values as the ligand cis to the nitrosyl group is varied.[20] The initial reduction of $[(tpy)(bpy)Os(NO)]^{3+}$ ($E_{1/2} = -0.02$ V) occurs at a potential 0.47 V more reducing than for $[(tpy)(bpy)Ru(NO)]^{3+}$ ($E_{1/2} = +0.45$ V). The origin of the decrease appears to be in a better energy match between $d\pi(Os(II))$ and $p\pi^*(NO^+)$, which leads to greater $d\pi$–$p\pi^*$ mixing for Os and more extensive back-donation of electron density from the metal to the nitrosyl ligand in $[(tpy)(bpy)Os(NO)]^{3+}$.

In water, the first reduction process for $[(tpy)(bpy)M(NO)]^{3+}$ is pH-independent and chemically reversible on the cyclic voltammogram time scale. In aqueous media the potentials are $E_{1/2} = 0.23$ V (M = Ru) and $E_{1/2} = -0.20$ V (M = Os). However, the cyclic voltammograms of $[(tpy)(bpy)Os(NO)]^{3+}$ in acidic

(28) Pipes, D. W.; Meyer, T. J. *J. Am. Chem. Soc.* **1984**, *106*, 7653–7654.

(29) Ehman, D. L.; Sawyer, D. T. *J. Electroanal. Chem. Interfacial Electrochem.* **1968**, *16*, 541.

solution appear more complicated than those of the ruthenium analogue. The shift to a more negative potential for the first reduction for M = Os (compared to the potential for M = Ru) leaves it sufficiently close to the subsequent, irreversible reduction waves that follow, that reversibility for this first reduction is lost.

The difference in $E_{1/2}$ values (Os vs. Ru) for the first wave of $[(tpy)(bpy)M(NO)]^{3+}$ in H_2O is 0.43 V, which compares well with the value observed in acetonitrile. Consequently, it is unlikely that any special stabilization of the oxidized form of either complex occurs in water compared to the case for acetonitrile.

Stage 2. In acetonitrile, the potentials for the second reduction of $[(tpy)(bpy)M(NO)]^{3+}$ are remarkably close, being −0.25 V for M = Ru and −0.24 V for M = Os. The second reduction process presumably occurs, once again, at largely $\pi^*(NO)$-based levels, to give $[(tpy)(bpy)M(NO)]^+$. The fact that the potentials are the same for the two metals might suggest that $d\pi-p\pi^*$ mixing is of less importance in the once-reduced complexes. However, this interpretation may be misleading as these potentials are influenced by a number of factors: (1) Reduction potential values depend upon the relative stabilization of both $[(tpy)(bpy)M(NO\cdot)]^{2+}$ and $[(tpy)(bpy)M(NO^-)]^+$. (2) Experimentally it is found that the potentials are solvent-dependent to differing degrees. Thus, in contrast to the similar values in CH_3CN, in aqueous solution M = Ru gives $E_p^c(B)$ = −0.36 V (pH 4.68), while for M = Os, $E_p^c(B)$ = −0.51 V (pH 9.15). The pH values chosen for comparison between the two couples are appropriate since the two couples are independent of pH in the respective pH regions. (3) Evidence is available for an intermediate stage, perhaps involving a linear-to-bent structural change at the nitrosyl ligand or chelate opening of tpy that probably precedes the actual charge-transfer step.

The evidence for an initial structural change to a new form capable of further reduction comes from (1) the plot of $i_p/v^{1/2}$ vs. log v for $[(tpy)(bpy)Ru(NO)]^{3+}$ in acetonitrile shown in Figure 4 and (2) the fact that in pH regions where the waves are independent of pH, the peak currents for the second and third reductions are noticeably smaller than peak currents for the first reduction, e.g. $i_p^c(A)/i_p^c(B) > 1$, and the ratio is sweep-rate-dependent. Presumably, at the scan rates shown in Figures 5 and 9 (100 mV/s), the rate of the structural change is comparable to the rate of charge transfer, leading to incomplete reduction of $[(tpy)(bpy)M(NO)]^{2+}$ because of the relative slowness of required structural rearrangement. With this interpretation the initial structural change gives a new form that is activated toward further reduction.

For the Ru complex, the second reduction at $E_p^c(B)$ = −0.36 V is relatively well-defined and pH-independent over the pH range 2.66–5.29. As shown in Figure 6 at pH 4.68, when the potential is held at the onset of the second reduction wave, clear evidence for an intermediate (I) is obtained, which reoxidizes at E_p^a = 0.47 V. Reoxidation of this intermediate occurs by two electrons to return to the nitrosyl complex. From the pH dependences of $E_p^a(I)$ in Figure 7, the reoxidation step also involves loss of a proton, suggesting that the overall process is

$$[(tpy)(bpy)Ru(NHO)]^{2+} \xrightarrow[-H^+]{-2e^-} [(tpy)(bpy)Ru(NO)]^{3+}$$

It necessarily follows that, in the range pH 2.66–5.29, the second reductive step must be followed by a proton-addition step and the overall reductive scheme in this pH range must be

$$[(tpy)(bpy)Ru^{II}-NO\cdot]^{2+} \rightleftharpoons [(tpy)(bpy)Ru(NO)]^{2+} \xrightarrow[\text{intermediate}]{+e^-}$$
$$[(tpy)(bpy)Ru(NO)]^+ \xrightarrow{+H^+} [(tpy)(bpy)Ru(NHO)]^{2+}$$

It is interesting to note that the same overall pattern of reduction events is maintained for $[(tpy)(bpy)Os(NO)]^{2+}$, although the pH ranges are shifted. For the Os complex at pH 8.18 or 9.15, i_p^c for the second wave at E_p^c = −0.51 V is pH-independent and is noticeably decreased in height (scan rate 100 mV/s) compared to i_p^c for the first wave. Between pH 8.18 and 6.80, the wave at E_p^c = −0.51 V disappears to be replaced by a wave of greatly enhanced peak height at E_p^c = −0.66 V.

Presumably, at pH 8.18, the second reduction proceeds by initial isomerization:

$$[(tpy)(bpy)Os^{II}-NO\cdot]^{2+} \rightarrow [(tpy)(bpy)Os(NO)]^{2+} \xrightarrow{+e^-}$$
$$[(tpy)(bpy)Os(NO)]^+$$

However, it is interesting to note from Figures 9 and 12 that no evidence for the appearance of an analogue of $[(tpy)(bpy)Ru(NHO)]^{2+}$ is obtained at pH 8.18, although a product wave for $[(tpy)(bpy)Os(NH_3)]^{2+}$ does occur at E_p^a = 0.41 V. It is likely that, at these elevated pH values, protonation of the nitrosyl ligand in $[(tpy)(bpy)Os(NO)]^+$ is too slow to compete with reoxidation or further reduction to give the ammine product. However, given the dramatic shift in potential and enhanced peak current seen at pH 6.8, a proton-induced further reduction of $[(tpy)(bpy)Os(NO\cdot)]^{2+}$ must occur that is relatively facile:

$$[(tpy)(bpy)Os(N{=}O\cdot)]^{2+} + H^+ \xrightarrow{+e^-}$$
$$[(tpy)(bpy)Os(NHO)]^{2+}$$

It is also interesting to note that, at pH 6.8, evidence for an intermediate with E_p^a = −0.11 V is obtained, which may be $[(tpy)(bpy)Os(NHO)]^{2+}$.

There is precedence for the linear-to-bent isomerization and for loss of a ligand upon reduction as noted earlier for nitroprusside. Linear-to-bent isomerization has been observed in intramolecular, two-electron-transfer processes involving d^6 nitrosyl complexes. Normally the intramolecular reactions are induced by addition of a Lewis base to a coordinatively unsaturated d^8 nitrosyl complex. Enemark, Feltham, et al.[30] have investigated the stepwise formation of a M(NHO) complex based on a linear-to-bent isomerization induced by initial anion binding (das is *o*-phenylenebis(dimethylarsine), *o*-$(Me_2As)_2C_6H_4$; X = NCS^-, Br^-):

$$[(das)_2Co^{I}{-}NO]^{2+} \underset{-X^-}{\overset{+X^-}{\rightleftharpoons}} [(das)_2XCo^{I}{-}NO]^+$$

$$[(das)_2XCo^{I}{-}NO]^+ \rightleftharpoons \left[(das)_2XCo^{III}{-}N{=}O\right]^+$$

$$\left[(das)_2XCo^{III}{-}N{=}O\right]^+ + H^+ \rightarrow [(das)_2XCo^{III}(NHO)]^{2+}$$

The formal similarity between the Co case and the reduction processes reported here can be appreciated by viewing the addition of the X^- ligand as involving anion binding and donation of an electron pair to the metal, in contrast to two-electron reduction at the nitrosyl:

$$[(tpy)(bpy)M^{II}(NO^+)]^{3+} \xrightarrow{2e^-} [(tpy)(bpy)M^{II}(NO^-)]^+$$

In either case, the product contains a six-coordinate, d^6 metal center bound to a NO^- ligand, at least in the formal sense. It is interesting to note that, for the Ru and Os nitrosyl complexes, a significant change in charge distribution occurs at the NO group even for the first reduction. $\bar{\nu}$(NO) decreases from 1970 to 1665 cm^{-1} when, for example, $[(bpy)_2(CH_3CN)Ru(NO)]^{3+}$ is reduced to $[(bpy)_2(CH_3CN)Ru(NO)]^{2+}$.[20]

The linear-to-bent interconversion or tpy chelate ring opening appears to "trigger" the further reductions at higher pH values, where the second and third reductions are pH-independent. Under these conditions, the diminished reductive peak currents for the second and third waves are consistent with two further one-electron reductions of $[(tpy)(bpy)Ru^{II}(NO\cdot)]^{2+}$:

$$[(tpy)(bpy)M^{II}(NO\cdot)]^{2+} \xrightarrow{+e^-} [(tpy)(bpy)M^{II}(NO)]^+$$

$$[(tpy)(bpy)M^{II}(NO)]^+ \xrightarrow{+e^-} [(tpy)(bpy)M(NO)]^0$$

(30) Enemark, J. H.; Feltham, R. D.; Riker-Nappier, J.; Bizot, K. F. *Inorg. Chem.* **1975**, *14*, 624.

Without corroborative spectral evidence, which is currently unobtainable, the assignment of electronic distributions within $[(tpy)(bpy)M(NO)]^+$ or $[(tpy)(bpy)M(NO)]^0$ is not possible.

There is some evidence—enhancement of the second and third reductions, disappearance of intermediates—that direct reduction of $[(tpy)(bpy)Ru^{II}(NO\cdot)]^{2+}$ may occur in acidic solutions (pH 1.41 for Ru and pH 2.96 for Os). It is conceivable that in sufficiently acidic solution the singly reduced complex may be protonated

$$[(tpy)(bpy)M(NO\cdot)]^{2+} + H^+ \rightleftharpoons [(tpy)(bpy)M(NOH\cdot)]^{3+}$$

and reduced directly

$$[(tpy)(bpy)M(NOH\cdot)]^{3+} \xrightarrow{e^-} [(tpy)(bpy)M(NHO)]^{2+}$$

with the necessity of a prior rearrangement.

Complexes with well-characterized, bent nitrosyl groups usually contain d^6 metals, and the nitrosyl ligand is best regarded at NO^-.[24,31] Characteristically, such complexes are subject to electrophilic attack akin to the protonation steps suggested above for $[(tpy)(bpy)M(NO^-)]^+$. For example, Roper et al. have reported that the reaction between $Os(Cl)(CO)(NO)(P(C_6H_5)_3)$ and 1 mol of HCl yields $OsCl_2(CO)(NHO)(P(C_6H_5)_3)_2$,[32] the structure of which was verified by Ibers and Wilson using X-ray techniques as containing the group[33]

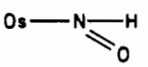

Protonation following the first reduction stage has also been suggested for the nitroprusside ion, where prior protonation[23]

$$[(CN)_5Fe^{II}(NO\cdot)]^{3-} + H^+ \rightleftharpoons [(CN)_5Fe^{II}(NHO)]^{2-}$$

is necessary for further reduction to occur. Direct polarographic reduction of $[(CN)_5Fe(NO^+)]^{2-}$ to $[(CN)_5Fe(NH_2OH)]^{3-}$ has also been reported to occur in solutions of sufficient acidity that protonation can assist the reduction steps.[23] It is also interesting to note that, in solutions of pH between 5 and 7, nitric oxide is reduced to N_2O,[29] and the mechanism proposed to account for the electrochemical data is

$$NO + H^+ \rightleftharpoons NOH^+$$

$$NOH^+ + e^- \rightarrow NOH$$

$$2NOH \rightarrow N_2O + H_2O$$

Electrochemical reduction of $[(tpy)(bpy)Ru(NO)]^{3+}$ in acetonitrile has certain similarities with reduction in water, but there are differences, and they are revealing. The products of reduction past the $[(tpy)(bpy)Ru(NO)]^{2+}$ stage with $n = 0.79$–1.0 are $[(tpy)(bpy)Ru(CH_3CN)]^{2+}$, $[(tpy)(bpy)Ru(NO_2)]^+$, and an intermediate with $E_p^a = 0.53$ V (0.1 M TEAP as supporting electrolyte). Note from Figure 3 that E_p^a for this intermediate is very near E_p^a for oxidation of $[(tpy)(bpy)Ru(NO\cdot)]^{2+}$ and further that oxidation of the intermediate leads to $[(tpy)(bpy)Ru(NO^+)]^{3+}$ as shown clearly by the appearance of the second nitrosyl reduction following an oxidative sweep. Both of these features were characteristic of $[(tpy)(bpy)Ru(NHO)]^{2+}$ in water. As in water, the intermediate is almost surely $[(tpy)(bpy)Ru(NHO)]^{2+}$, which undergoes a two-electron oxidation to return to $[(tpy)(bpy)Ru(NO)]^{3+}$.

Of the two remaining products, the appearance of the nitro complex is most revealing since it signals what must be an intermediate disproportionation step:

$$2[(tpy)(bpy)Ru(NO^-)]^+ \rightarrow [(tpy)(bpy)Ru(NO_2)]^+ + [(tpy)(bpy)Ru(N)]^+$$

It is necessary to invoke a disproportionation step in order to explain how a ligand-based reduction from $[(tpy)(bpy)Ru(NO\cdot)]^{2+}$ to $[(tpy)(bpy)Ru(NO^-)]^+$ can lead to a net oxidation at the ligand. The disproportionation reaction is reminiscent of the chemistry that occurs upon oxidation of the corresponding Ru^{II}–NO_2 complex to Ru^{III}–NO_2:[21]

$$2[(tpy)(bpy)Ru(NO_2)]^+ \xrightarrow{-2e^-} 2[(tpy)(bpy)Ru(NO_2)]^{2+} \rightarrow [(tpy)(bpy)Ru(NO)]^{3+} + [(tpy)(bpy)Ru(ONO_2)]^+$$

The key step in the overall reaction appears to be an oxo-transfer step from one Ru^{III}–NO_2 site to a second, but as the O-bound, nitrito isomer:

$$[(tpy)(bpy)Ru(NO_2)]^{2+} + [(tpy)(bpy)Ru(ONO)]^{2+} \rightarrow [(tpy)(bpy)Ru(NO)]^{3+} + [(tpy)(bpy)Ru(ONO_2)]^+$$

In a formal sense, the second product of a disproportionation of $[(tpy)(bpy)Ru(NO^-)]^+$ could be viewed as $[(tpy)(bpy)Ru^{II}(N^-)]^+$ or as $[(tpy)(bpy)Ru^{IV}(N^{3-})]^+$. In the latter formulation, the intermediate is simply the deprotonated form of $[(tpy)(bpy)Ru^{IV}(NH)]^{2+}$, which has been observed as an intermediate formed by disproportionation of $[(tpy)(bpy)Ru^{III}(NH_3)]^{3+}$.[11] It is appealing to invoke $[(tpy)(bpy)RuN]^+$ as an intermediate since it provides a basis for explaining $[(tpy)(bpy)Ru(CH_3CN)]^{2+}$ as a product via a coupling reaction to give a dinitrogen-bridged dimer

$$2[(tpy)(bpy)Ru^{IV}{\equiv}N]^+ \xrightarrow{-2e^-} [(tpy)(bpy)Ru^{II}(NN)Ru^{II}(bpy)(tpy)]^{4+}$$

followed by loss of N_2

$$[(tpy)(bpy)Ru^{II}(NN)Ru^{II}(bpy)(tpy)]^{4+} + 2CH_3CN \rightarrow 2[(tpy)(bpy)Ru(CH_3CN)]^{2+} + N_2$$

It should be noted that, in this coordination environment, dinitrogen complexes of Ru(II) are expected to be unstable with respect to the loss of N_2.[20,34]

Stage 3. A third reduction stage of $[(tpy)(bpy)M(NO)]^{3+}$ is clearly observed in aqueous solution. As noted earlier from pH dependences for the Ru complex, the product of the third reduction appears to have been reduced by three electrons and to have gained two protons and is probably therefore either $[(tpy)(bpy)Ru(N)]^{2+}$ or $[(tpy)(bpy)Ru(NH_2O)]^{2+}$, where the "hydrated" group could be either HNOH or NOH_2. There is precedence for the hydrated intermediate in the complex $OsCl_2(NO)(NHOH)(P(C_6H_5)_3)_2$, which has been isolated following the addition of 2 mol of HCl to $OsCl(NO)_2(P(C_6H_5)_3)_2$.[32]

It is important to note from Figure 5 that, above about pH 2, further reduction past stage 3 for the Ru complex does not occur on the cyclic voltammetry time scale (100 mV/s). Reductive scans past the third wave do not lead to the ammine product, but rather the reoxidation of an intermediate is observed at $E_p^a = +0.58$ V. However, coulometry studies show that this intermediate, either $[(tpy)(bpy)Ru(N)]^{2+}$ or $[(tpy)(bpy)Ru(NH_2O)]^{2+}$, is ultimately reduced to the ammine complex. The two observations suggest that direct reduction at the electrode is slow. It is interesting to note that in more strongly acidic solutions where the three-electron-reduced intermediate appears to be protonated—$[(tpy)(bpy)Ru(NH)]^{3+}$ or $[(tpy)(bpy)Ru(NH_2OH)]^{3+}$—the intermediates do not build up since they are reduced at the electrode to give the ammine product.

For the Os complex, the situation is related but different. There is no shift in E_p^c values between pH 8.18 and 9.15 for the second or third reduction waves, and scans through either do not lead to the appearance of intermediates. Presumably, in this pH range, further reduction of $[(tpy)(bpy)Os(NO\cdot)]^{2+}$ occurs by successive one-electron steps:

$$[(tpy)(bpy)Os(NO)]^{2+} + e^- \rightarrow [(tpy)(bpy)Os(NO)]^+$$

$$[(tpy)(bpy)Os(NO)]^+ + e^- \rightarrow [(tpy)(bpy)Os(NO)]^0$$

(31) Collman, J. P.; Hegedus, L. S. "Principles and Applications of Organotransition Metal Chemistry"; University Science Books: Mill Valley, CA, 1980; pp 148–149.
(32) Grundy, K. R.; Reed, C. A.; Roper, W. R. *J. Chem. Soc., Chem. Commun.* **1970**, 1501.
(33) Wilson, R. D.; Ibers, J. A. *Inorg. Chem.* **1979**, *18*, 336.
(34) Callahan, R. W. Ph.D. Dissertation, The University of North Carolina.

It is also significant that, at pH 8.18 or 9.15, potential scans past the third reduction produce the ammine product directly (E_p^a = 0.46 V at pH 8.18) even though *there is no evidence of further reduction* or for the appearance of the intermediates $[(tpy)(bpy)Os(NHO)]^{2+}$, $[(tpy)(bpy)Os(N)]^{2+}$, and $[(tpy)(bpy)Os(NH_2O)]^{2+}$. When they are taken together, these observations point toward a disproportionation step past the three-electron-reduced stage to give $[(tpy)(bpy)Os(NO)]^{3+}$ and $[(tpy)(bpy)Os(NH_3)]^{2+}$. By pH 6.80 the second reduction has become proton-dependent and $[(tpy)(bpy)Os(NHO)]^{2+}$ appears in the solution. Below pH 6.80 the third reduction becomes proton-dependent and overcomes the second reduction, resulting in a single, multielectron, multiproton wave that moves steadily to more positive potentials as the pH is lowered.

Pattern of Mechanistic Events in the Interconversion between the Nitro and Ammine Groups. The interconversion between nitrosyl and ammine complexes is reversible in the net sense, e.g.

$$H_2O + [(tpy)(bpy)Ru(NH_3)]^{2+} \underset{+6e^-,\,+5H^+}{\overset{-6e^-,\,-5H^+}{\rightleftharpoons}} [(tpy)(bpy)Ru(NO)]^{3+}$$

which allows mechanistic information to be obtained starting with either the oxidation of $[(tpy)(bpy)M(NH_3)]^{2+}$ or the reduction of $[(tpy)(bpy)M(NO)]^{3+}$ (M = Ru, Os). The overall pattern of redox events is basically the same for Ru(II) and Os(II) in that they appear to involve a series of one-electron steps, but differences do appear in shifts in redox potentials and in acid–base properties.

On the oxidative side, the key to oxidation past the M(II) → M(III) stage appears to be the presence of kinetically significant amounts of the amido complex $[(tpy)(bpy)M^{III}(NH_2)]^{2+}$. For M = Ru, further oxidation of $[(tpy)(bpy)Ru(NH)]^{2+}$ and successive intermediates occurs at less positive potentials and a multielectron oxidation wave to give $[(tpy)(bpy)Ru(NO)]^{3+}$ is observed. For M = Os, an oxidative wave for the Os(III/IV) step is observed, but the absence of a return wave shows that, once formed, Os(IV) is unstable.

On the reductive side the first key is the initial nitro to nitrosyl, acid–base interconversion

$$[(tpy)(bpy)M(NO_2)]^+ \underset{-H_2O}{\overset{2H^+}{\longrightarrow}} [(tpy)(bpy)M(NO)]^{3+}$$

which creates low-lying, largely $\pi^*(NO)$ levels at which the reductive process is initiated. The first step is chemically reversible

$$[(tpy)(bpy)M(NO^+)]^{3+} + e^- \rightleftharpoons [(tpy)(bpy)M(NO\cdot)]^{2+}$$

but the second appears to be complicated by a structural change that occurs on the cyclic voltammetry time scale. The resulting intermediate undergoes a second reduction followed by a protonation to give $[(tpy)(bpy)M(NHO)]^{2+}$. By pH 6.80 for M = Os, a proton-dependent pathway exists for the direct formation of $[(tpy)(bpy)Os(NHO)]^{2+}$.

Once formed, the intermediate $[(tpy)(bpy)Ru(NHO)]^{2+}$ undergoes a further one-electron, one-proton reduction to give $[(tpy)(bpy)Ru(N)]^{2+}$ or $[(tpy)(bpy)Ru(NH_2O)]^{2+}$. By contrast, for M = Os there is no evidence for the appearance of $[(tpy)(bpy)Os(N)]^{2+}$ or $[(tpy)(bpy)Os(NH_2O)]^{2+}$. In fact, below pH 6.80 not even $[(tpy)(bpy)Os(NHO)]^{2+}$ builds up in solution because it undergoes a further, proton-assisted reduction at a potential less negative than the potential for reduction of $[(tpy)(bpy)Os(NO\cdot)]^{2+}$.

The differences between the M = Ru and Os cases at this stage of reduction are significant and worthy of further comment. For M = Ru the buildup of the three-electron product suggests that the next stage in the reduction is slow. A possible explanation is that at this step a reductive "dehydration" occurs

$$[(tpy)(bpy)Ru^{II}(NH_2O)]^{2+} \underset{-H^+,\,-e^-}{\overset{+H^+,\,+e^-}{\rightleftharpoons}} [(tpy)(bpy)Ru^{IV}(NH)]^{2+} + H_2O$$

Scheme I

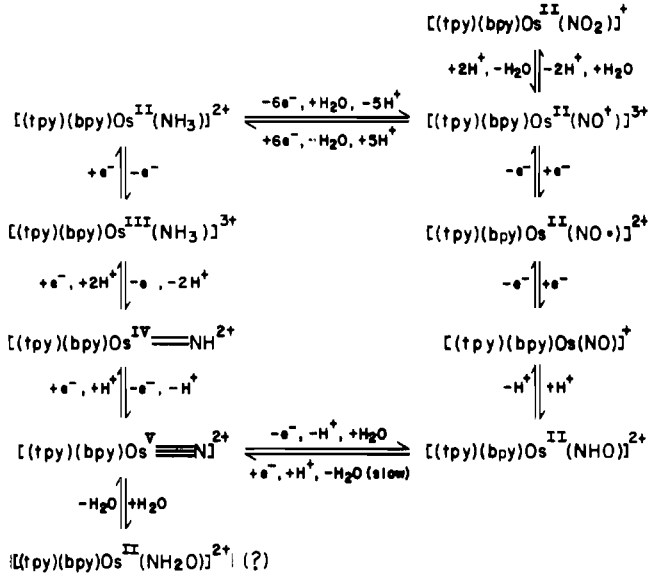

which is slow because of the complexity of the step. On the other hand, the appearance of only $[(tpy)(bpy)Os(NHO)]^{2+}$ as an intermediate suggests that a conversion of this type occurs at the third rather than the fourth stage of reduction

$$[(tpy)(bpy)Os^{II}(NHO)]^{2+} \underset{-H^+,\,-e^-}{\overset{+H^+,\,+e^-}{\rightleftharpoons}} [(tpy)(bpy)Os^{V}(N)]^{2+} + H_2O$$

followed by facile reduction of $[(tpy)(bpy)Os^V(N)]^{2+}$ via $[(tpy)(bpy)Os^{IV}(NH)]^{2+}$ and $[(tpy)(bpy)Os(NH_3)]^{3+}$.

That there might be a fundamental difference between the dominant forms of the Os and Ru intermediates in equivalent coordination environments is not surprising, given, for example, the relative plethora of higher oxidation state nitrido complexes of Os and the paucity of Ru examples. The situation with regard to the proposed hydration–dehydration steps is entirely analogous to the reaction between $[(tpy)(bpy)Ru^{IV}{=}NH]^{2+}$ and water to give $[(tpy)(bpy)Ru^{II}(NH_2OH)]^{2+}$.

The circumstances with regard to the hydration–dehydration reactions may vary with pH. For example, the cyclic voltammogram of $[(tpy)(bpy)Ru(NO)]^{3+}$ at pH 1.41 (Figure 5a) shows that at this pH $[(tpy)(bpy)Ru(NH_3)]^{2+}$ appears at the expense of $[(tpy)(bpy)Ru(NHO)]^{2+}$ and of the three-electron intermediate. Also, note that there is a decrease in peak current and a shift in peak potential for the three-electron intermediate. Under these conditions it is conceivable that the dehydrated intermediates may begin to play a role if only as kinetic intermediates in steps like

$$H^+ + [(tpy)(bpy)Ru^{II}(NHO)]^{2+} \rightleftharpoons [(tpy)(bpy)Ru^{VI}(N)]^{3+} + H_2O$$

$$[(tpy)(bpy)Ru^{VI}(N)]^{3+} \underset{-e^-}{\overset{+e^-}{\rightleftharpoons}} [(tpy)(bpy)Ru^{V}(N)]^{2+}$$

$$H^+ + [(tpy)(bpy)Ru^{V}(N)]^{2+} \underset{-e^-}{\overset{+e^-}{\rightleftharpoons}} [(tpy)(bpy)Ru^{IV}(NH)]^{3+}$$

$$H^+ + [(tpy)(bpy)Ru^{II}(NH_2O)]^{2+} \rightleftharpoons [(tpy)(bpy)Ru^{V}(NH)]^{3+} + H_2O$$

An appealing feature of an interpretation invoking hydrated intermediates, at least at higher pH values, is that the waves that characterize the intermediates at E_p^a = 0.58 and 0.46 V (pH 4.66) then represent a natural sequence of ligand-based oxidations through the series of complexes $[(tpy)(bpy)Ru(NH_3)]^{2+}$, $[(tpy)(bpy)Ru(NH_2OH)]^{2+}$, $[(tpy)(bpy)Ru(NH_2O)]^{2+}$, $[(tpy)(bpy)Ru(NHO)]^{2+}$, and $[(tpy)(bpy)Ru(NO)]^{3+}$, which includes all of the expected stages in the transformation of bound NH_3 into NO^+. It should be realized that the alternate formu-

Scheme II

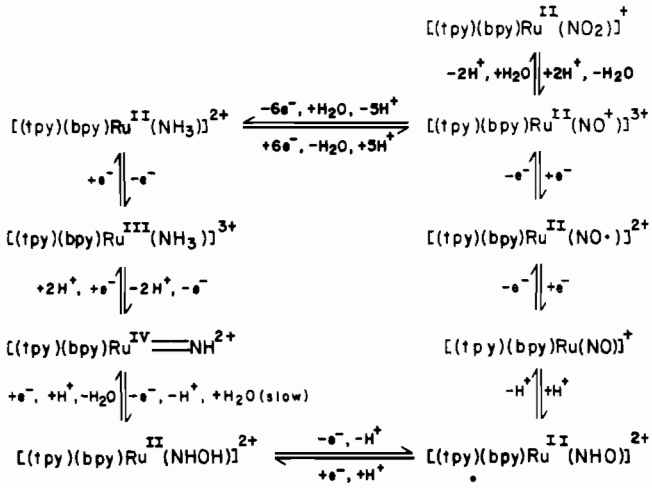

lations of the intermediates proposed here which differ with regard to water content, e.g., $[(tpy)(bpy)Ru^{II}(NH_2O)]^{2+}$ vs. $[(tpy)(bpy)Os^{V}{\equiv}N]^{2+}$, may be profound with regard to both electronic structure and reactivity characteristics. For example, the spectral properties of $[(tpy)(bpy)Ru^{IV}{=}NH]^{2+}$ are essentially those of the high-oxidation-state oxo complex $[(tpy)(bpy)Ru^{IV}{=}O]^{2+}$, which features an absence of visible absorption bands.[11b] The "reductive hydration" reaction

$$[(tpy)(bpy)Ru^{IV}{=}NH]^{2+} + H_2O \rightarrow [(tpy)(bpy)Ru^{II}(NH_2OH)]^{2+}$$

produces a typical complex of Ru(II) having intense metal to ligand charge-transfer (MLCT) absorption bands (π^*(bpy) ← $d\pi(Ru^{II})$) at nearly the same energy as for the ammine complex $[(tpy)(bpy)Ru(NH_3)]^{2+}$.[11] The presence or absence of hydrated–dehydrated pairs like $M^{IV}{=}NH^{2+}/M^{II}{-}NH_2OH^{2+}$, $M^{V}{\equiv}N^{2+}/M^{II}{-}NH_2O^{2+}$, and $M^{IV}{=}N^{+}/M^{II}{-}NHO^{2+}$ may depend on the pH, the metal, and the ligand environment involved, and we hope to learn how to control this chemistry in a systematic way.

In Schemes I and II an attempt has been made to summarize our best guesses as to the mechanistic details for the nitro–ammine interconversion for the Ru and Os complexes in the pH range 2–6.

Acknowledgment is made to the National Institutes of Health under Grant No. 5-RO1-GM32296-02 for support of this research.

Contribution from the Gibbs Chemical Laboratory, Department of Chemistry, Harvard University, Cambridge, Massachusetts 02138

Structures and Energies of B_2H_4

R. Ricki Mohr and William N. Lipscomb*

Received November 18, 1985

Optimized structures and energies have been determined at the HF/6-31G and MP2/6-31G** levels for B_2H_4. At the MP2/6-31G** level the optimized BB distances are 1.653 Å for the orthogonal 0012 D_{2d} structure, 1.537 Å for the 1011 C_s structure (BH_2 perpendicular to BHBH plane), and 1.462 Å for the doubly bridged 2010 C_{2v} structure. The C_s and C_{2v} structures are less stable than the D_{2d} structure by 9.6 and 1.5 kcal/mol, respectively. The barrier for rotation of the D_{2d} form through the planar 0012 D_{2h} form (**BB**, 1.742 Å) is 12.6 kcal/mol, while the barrier for inversion of the 2010 C_{2v} form through the planar 2010 D_{2h} form (**BB**, 1.493 Å) is 19.0 kcal/mol.

Although B_2H_4 is unknown, it is of theoretical interest[1-8] and has been proposed in interconversion reactions of boranes.[9] It is among the simplest models of a classical to nonclassical transformation in which terminal hydrogens could potentially become bridge hydrogens, thus using the vacant orbital on each BH_2 group of the classical structure. Here we show that, although the classical H_2BBH_2 (D_{2d}) structure is more stable than the nonplanar doubly bridged structure, only 1.5 kcal/mol separates these two structures (Figure 1).

In earlier studies optimized geometries have been found by various methods: FSGO (floating spherical Gaussian orbitals),[1] PRDDO (partial retention of diatomic differential overlap),[2] single-ζ[3,4] and double-ζ[5-7] methods (Table I). The D_{2d} classical structure H_2BBH_2 is found in these studies to be more stable than the planar $HB(H_b)_2BH$ structure of symmetry D_{2h} (Table II). Experimentally, classical forms (D_{2d} or D_{2h}) are known[10] for B_2F_4, B_2Cl_4, and B_2Br_4. Perhaps for these reasons, the more extensive calculations on B_2H_4 have been concentrated on the D_{2d} and D_{2h} classical structures and on the rotational barrier. Polarization functions have been added for single geometry calculations[3] and double-ζ plus polarization basis sets including CI (configuration interaction) used in optimization of the preferred H_2BBH_2 (D_{2d}) isomer[7] (Table II). Comparisons have also been made of the planar 0012 (D_{2h}) and 2010 (D_{2h}) structures and of the barrier

(1) Blustin, P. H.; Linnett, J. W. *J. Chem. Soc., Faraday Trans. 2* **1975**, *71*, 1058.
(2) Pepperberg, I. M.; Halgren, T. A.; Lipscomb, W. N. *Inorg. Chem.* **1977**, *16*, 363.
(3) Dill, J. D.; Schleyer, P. v. R.; Pople, J. A. *J. Am. Chem. Soc.* **1975**, *97*, 3402.
(4) Bigot, A. B.; Lequan, R. M.; Devaquet, A. *Nouv. J. Chem.* **1978**, *2*, 449.
(5) McKee, M. L.; Lipscomb, W. N. *J. Am. Chem. Soc.* **1981**, *103*, 4673.
(6) Armstrong, D. R. *Inorg. Chim. Acta* **1976**, *18*, 13.
(7) Vincent, M. A.; Schaefer, H. F. *J. Am. Chem. Soc.* **1981**, *103*, 5677.
(8) Halova, O. *Sb. Vys. Sk. Chem.-Technol. Praze, Fyz. Mater. Merici Tech.* **1983**, *P6*, 35.
(9) Massey, A. G. *Chem. Br.* **1980**, *16*, 588. Rathke, J.; Schaefer, R. *Inorg. Chem.* **1974**, *13*, 760. von Doorne, W.; Cordes, A. W.; Hunt, G. W. *Inorg. Chem.* **1973**, *12*, 1686.
(10) Danielson, D. D.; Patton, J. V.; Hedberg, K. *J. Am. Chem. Soc.* **1977**, *99*, 6484. Trefonas, L.; Lipscomb, W. N. *J. Chem. Phys.* **1958**, *28*, 54. Jones, L. H.; Ryan, R. R. *J. Chem. Phys.* **1972**, *57*, 1012. Ryan, R. R.; Hedberg, K. *J. Chem. Phys.* **1969**, *50*, 4986. Atoji, M.; Wheatley, P. J.; Lipscomb, W. N. *J. Chem. Phys.* **1957**, *27*, 196. Danielson, D. D.; Hedberg, K. *J. Am. Chem. Soc.* **1979**, *101*, 3199.

0020-1669/86/1325-1053$01.50/0